Integrating climatic information in water resources modelling and optimisation

Gelati, Emiliano; Rosbjerg, Dan; Madsen, Henrik

Publication date:
2010

Document Version
Publisher's PDF, also known as Version of record

Technical University of Denmark

Integrating climatic information in water resources modelling and optimisation

Emiliano Gelati

DTU Environment
Department of Environmental Engineering

PhD Thesis
September 2010

Integrating climatic information in water resources modelling and optimisation

Emiliano Gelati

PhD Thesis
September 2010

Department of Environmental Engineering
Technical University of Denmark

Emiliano Gelati

Integrating climatic information in water resources modelling and optimisation

PhD Thesis, September 2010

The thesis will be available as a pdf-file for downloading from the homepage of the department: www.env.dtu.dk

Address:	DTU Environment Department of Environmental Engineering Technical University of Denmark Miljoevej, building 113 DK-2800 Kgs. Lyngby Denmark
Phone reception:	+45 4525 1600
Phone library:	+45 4525 1610
Fax:	+45 4593 2850
Homepage:	http://www.env.dtu.dk
E-mail:	reception@env.dtu.dk

Printed by:	Vester Kopi Virum, September 2010
Cover:	Torben Dolin
ISBN:	978-87-92654-09-0

Preface

The work reported in this PhD thesis, entitled "Integrating climatic information in water resources modelling and optimisation", was conducted at the Department of Environmental Engineering (Technical University of Denmark) and at DHI Water – Environment – Health, under the supervision of Dan Rosbjerg and Henrik Madsen. The PhD project ran from March 2007 to June 2010 and was funded by the Technical University of Denmark.

The content of the PhD thesis is based on four papers prepared for scientific journals. In the text, the papers are referred to by their appendix number written with roman numbers.

I. Gelati, E., O. B. Christensen, P. F. Rasmussen, and D. Rosbjerg, Downscaling atmospheric patterns to multi-site precipitation amounts in southern Scandinavia, *Hydrology Research*, *41*(3-4), 193–210, doi: 10.2166 / nh.2010.114, 2010.

II. Gelati, E., H. Madsen, and D. Rosbjerg, Markov-switching model for non-stationary runoff conditioned on El Niño information, *Water Resources Research*, *46*, W02517, doi: 10.1029 / 2009WR007736, 2010.

III. Gelati, E., H. Madsen, and D. Rosbjerg, Stochastic reservoir optimisation using El Niño information – case study of Daule Peripa, Ecuador, revised to *Hydrology Research*.

IV. Gelati, E., H. Madsen, and D. Rosbjerg, Reservoir operation using El Niño forecasts, submitted manuscript.

The papers are not included in this www-version, but can be obtained from the Library at DTU Environment:
Department of Environmental Engineering
Technical University of Denmark
Miljøvej, Building 113
DK-2800 Kongens Lyngby, Denmark
(library@env.dtu.dk)

Acknowledgements

I would like to thank my supervisors, *Dan Rosbjerg* and *Henrik Madsen*, for their good guidance.

I would also like to thank *Anders*, *Annette*, and *Gitte*, for having been good office mates during these years.

My work would have been much less inspired without the good lunches and breaks with *Flavio*, *Gianluca*, and *José*. Many thanks to them, for being good colleagues and friends.

My gratitude goes to *Alberto*, *Alessio*, *Elena*, *Emanuele*, and *Ole* for having been good friends here in Copenhagen.

I am also grateful to all my friends in *Castano Primo*, *Milano*, and *Madrid*, for having made me feel at home each time I went there.

My largest acknowledgement is for my parents, *Franco* and *Nunzia*, who provided me with strength and motivation to face this and any other challenge in life.

Summary

Water resources modelling and optimisation methods need to include climatic information, in order to be applied to problems where climatic variability is an important factor. In this study, stochastic modelling and optimisation methods using climatic information are defined, combined and applied to water resources applications.

The presented modelling approaches assume the hydrologic variables to depend on an unobservable state variable representing the prevailing climatic conditions. The hidden state is assumed to shift between a finite number of values according to a Markov chain, whose transition probabilities are functions of climatic information. Thus the hidden state process mimics climate-induced hydrologic regime shifts. This general modelling framework is applied to two case studies, by defining an appropriate conditional description of the hydrologic variables for each case.

In the first case study, the probability distribution of multi-gauge daily precipitation amounts in southern Scandinavia is conditioned on a hidden weather state, whose transitions are influenced by gridded atmospheric variables. The high-dimensional atmospheric fields are summarized via singular value decomposition, which preserves most of the covariance with precipitation. To account for the spatial dependence structure of precipitation while limiting the growth of model dimension, the conditional multivariate probability distributions of precipitation occurrences are approximated by Chow-Liu trees. Given the weather state and the precipitation occurrence pattern, amount distributions are modelled independently at each gauge. The model yields robust predictions of precipitation statistics. The 8 identified weather states are consistent with the weather types of the study area. Chow-Liu trees improve the reproduction of the spatial correlation of precipitation compared to assuming conditional spatial independence. However, an explicit parameterisation of the spatial dependence structure of precipitation amounts may bring further improvement.

In the second case study, monthly inflow anomalies of the Daule Peripa and Baba reservoirs (in Ecuador) are modelled by a mixture of autoregressive models with exogenous input (ARXs), each one corresponding to a hidden climate state. El Niño – Southern Oscillation (ENSO) indices are used both to compute state transition probabilities and as exogenous covariates. Thus the hidden climate state pro-

cess represents ENSO-induced inflow regime shifts, and the ARXs account directly for the influence of ENSO. The model generates realistic simulated and forecasted inflow scenarios based on, respectively, historical records and forecasts of ENSO indices. ENSO forecasts are currently published with 9 month lead time. Of the 2 identified climate states, one corresponds to El Niño and the other represents both La Niña and normal conditions. Indeed El Niño is well correlated with anomalously high inflow, while La Niña does not have a significant impact on inflow. Consistently, large positive anomalies are reasonably predicted, while anomalously low inflow is generally overestimated. To improve drought prediction, climatic indices correlating with negative inflow anomalies should be pursued.

The presented optimisation methods use time series generated by the climate-driven hydrologic models as stochastic input. They are applied to the Daule Peripa – Baba reservoir system, which supplies hydropower plants and downstream water users. We follow the simulation-optimisation approach, by coupling a genetic algorithm with a simulation model of the reservoir system. To account for input uncertainty, sampling objective functions are evaluated by simulating the water resources system with ENSO-based synthetic inflow scenarios. Long-term optimisation (LT) calibrates rule curves that return reservoir releases as functions of storage and season, using long simulated inflow scenarios. Short-term optimisation (ST) is performed at the beginning of each month, and determines releases using inflow forecasts and seasonal storage targets. Both LT and ST outperform the historical management of Daule Peripa. In particular ST yields the best results, as it combines short- and long-term information. Despite the promising results obtained by applying ST to the planned Daule Peripa – Baba reservoir system, further research should be conducted on flood prevention during intense El Niño events.

The presented methods might be used to assess the consequences of global climate change scenarios on water resources systems that need small-scale hydrologic data as input. However, such assessments may be affected by large or even unquantifiable uncertainties, as methods calibrated under past climatic conditions might not be valid under altered climate scenarios.

Dansk sammenfatning

Når det drejer sig om problemstillinger, hvor klimavariabiliteten er en vigtig faktor, bør information om lokale klimasvingninger medtages i vandressource-modellering og -optimering. I afhandlingen er stokastiske modellerings- og optimeringsmetoder, der inddrager klimainformation, defineret, kombineret og anvendt i en vandressource-sammenhæng.

De præsenterede modeller har som antagelse, at de hydrologiske variable afhænger af en ikke-målbar tilstandsvariabel, der repræsenterer den fermherskende klimatilstand. Den skjulte klimatilstand antages at skifte mellem et endeligt antal værdier svarende til en Markov-kæde, hvis overgangssandsynligheder er funktioner af den klimatiske information. På den måde afspejler den skjulte tilstandsproces observerbare klima-inducerede ændringer i det hydrologiske regime. Den overordnede modellerings-ramme er anvendt på to forskellige eksempler.

I det første tilfælde er sandsynligheds-fordelingen for den simultane nedbør på en lang række nedbørsstationer i de sydlige Skandinavien betinget af en skjult vejrtilstand, hvor overgangssandsynligheden fra én tilstand til en anden afhænger af grid-værdier af atmosfæriske variable. De flerdimensionale atmosfæriske variable kunne reduceres væsentligt ved hjælp af SVD (singular value decomposition), hvorved kovariansen til nedbøren kun blev marginalt berørt. Den rumlige afhængighedsstruktur i nedbørs-processen er modelleret med Chow-Liu træer, hvil-ket kun giver en begrænset vækst i model-dimensionen. For en given vejrtilstand og nedbørsmønster opnås herved robuste sandsynlighedsfordelinger for nedbørs-mængden på de forskellige stationer. Modellen identificerer 8 vejrtilstande, som giver et konsistent billede af de fremherskende vejrtyper i området. Chow-Liu træer forbedrer reproduktionen af den rumlige korrelation i sammenligning med en antagelse om rumlig uafhængighed. En eksplicit parametrisering af afhængigheds-strukturer må imidlertid formodes at lede til yderligere forbedringer.

I det andet eksempel er månedlige anomalier af indstrømningen til to reservoirer i Ecuador, Daule Peripa og Baba, modelleret ved hjælp af en blanding af autoregressive modeller med eksogent input, hvor de enkelte modeller hver svarer til en skjult klimatilstand. Indekser for El Niño Southern Oscillation (ENSO) er benyttet både til at beregne overgangssandsynlighederne og som eksogene kovarianter. De skjulte klimatilstande repræsenterer således ENSO-inducerede regime-

skift i indstrømningen. Denne ENSO-indflydelse tages direkte i regning af ARX-modellerne, der genererer realistiske simuleringer og forudsigelser af indstrømnings-scenarier baseret på henholdsvis observationer og forudsigelser af ENSO-indekser. ENSO-forudsigelser publiceres løbende med en 9 måneders tidshorisont. To forskellige klimatilstande er identificeret, én svarende til El Niño-situationen, mens den anden repræsenterer både La Niña- og normal-tilstanden. El Niño korresponderer meget fint til unormalt høje indstrømninger, hvorimod La Niña ikke synes at have nogen væsentlig indflydelse på indstrømningen. Det betyder, at høje indstrømninger er godt prædikterede, mens særligt lave indstrømninger generelt er overestimerede. En forbedring af tørke-forudsigelser vil kræve, at der kan findes klima-variable, der korrelerer til negative indstrømnings-anomalier, hvilket hidtil ikke er lykkedes.

De præsenterede optimerings-metoder benytter tidsserier genereret af den klimadrevne hydrologiske model som stokastisk input. Disse er anvendt på Daule Peripa-Baba reservoir-systemet, som forsyner vandkraftturbiner og nedstrøms vandbrugere. Der benyttes en simulerings-optimerings tilgang ved at koble en genetisk algoritme (heuristisk optimeringsmodel) til en simuleringsmodel for reservoir-systemet. Input-usikkerheden tages i regning gennem sampling målfunktioner, der beregnes og minimeres under anvendelse af de ENSO-baserede syntetiske indstømnings-scenarier. Langtids-optimering kalibrerer styrekurver, der bestemmer reservoir-udstrømningen som funktion af vandindhold og årstid ved hjælp af lange simulerede indstrømnings-serier. Korttids-simulering beregner for en 9-måneders horisont den optimale reservoir-udstrømning under anvendelse af syntetiske indstrømnings-serier baseret på El Niño -forudsigelser og de sæsonmæssige mål for reservoir-indholdet begegnet af langtidssimuleringen. Den optimerede udstrømning anendes for den første af de 9 måneder, hvorefter korttids-optimeringen gentages et tidsskridt senere, etc. Både langtids- og korttids-optimeringen giver forbedrede resultater i forhold til den historiske regulering, korttids-simuleringen i særdeleshed, idet den kombinerer både korttids- og langtids-information. På grund af det lille reservoirindhold i Baba bør der foretages yderligere undersøgelser af oversvømmelses-risikoen i forbindelse med intense El Niño-situationer som forudsætning for implementering af de opnåede resultater.

De præsenterede metoder kunne muligvis anvendes til en bedømmelse af konsekvenserne af fremtidige globale klimavariationers påvirkning af vandressource-systemer, der kræver hydrologiske data på lille skala som input. Imidlertid må

det påregnes, at store og måske ukvantificerbare usikkerheder må tages i betragtning, da metoder kalibreret under de nuværende klimaforhold ikke nødvendigvis vil være gældende under væsentligt ændrede forhold.

Contents

1 Introduction

The interest in modelling hydrologic variables derives from the need of providing water resources simulation models with reliable input time series. Such interest has been notably enhanced by climate change predictions. Global climate models produce scenarios at large spatial scales, while hydrologic variables need to be predicted at local scale for assessing climate change impacts on water resources. Thus stochastic models can be used to translate large-scale information from physically-based climate models to small-scale hydrologic data. Traditional stationary stochastic approaches have not used climatic information to condition time series generation. It is widely acknowledged that models not including climatic input should not be applied under climatic conditions that differ from those of calibration. Therefore the development of stochastic hydrologic models accounting for the influence of climatic variability has become a priority. Furthermore, such models have to be complemented by methods that can effectively exploit the included climatic information for water resources optimisation.

The research work was aimed at developing stochastic hydrologic models and water resources optimisation methods that could yield benefits from including large-scale climatic information. In the first research application, we implemented a stochastic model to downscale large-scale atmospheric variables to precipitation amounts for a gauge dense network in southern Scandinavia. Then we developed a stochastic model using El Niño – Southern Oscillation (ENSO) information to describe reservoir inflow in Ecuador. Both proposed stochastic models are based on the assumption that the observable processes (precipitation or inflow) are conditioned on an unobservable state variable (weather or climate) shifting between a finite number of values. We investigated different innovative aspects of stochastic hydrologic modelling using climatic information: in the precipitation modelling study, we applied a spatial correlation model for multivariate precipitation; in the inflow modelling application, we accounted for the climatic influence on inflow by directly correlating ENSO indices with inflow anomalies. Finally, we defined several reservoir optimisation methods that could exploit the synthetic ENSO-based inflow scenarios produced by the inflow model. Thus we tested the benefits of using the developed modelling approach for reservoir optimisation.

In the remainder of this chapter, we first provide a literature review characterising the state of the art of the research areas of interest (see section 1.1); then we give

a brief overview of the proposed methods, placing them in the context of recent research developments (see section 1.2); and finally we outline the structure of the thesis (see section 1.3).

1.1 Literature review

Sections 1.1.1 and 1.1.2 review relevant scientific literature on, respectively, stochastic models for hydrologic time series and reservoir optimisation methods.

1.1.1 Review of stochastic models for hydrologic time series

Stochastic models are often used to generate synthetic time series of hydrologic variables, such as precipitation and streamflow. To realistically simulate water resources systems, model development is faced by the challenging task of accounting for climatic variability in the description of hydrologic variables. Traditional stochastic modelling approaches have not accounted for climatic variability, thus resulting in stationary descriptions. Though not including climatic information, many models have been developed to mimic the regime-like behaviour of hydrologic systems. Among the various approaches, Markovian processes deserved particular attention (*Hughes and Guttorp*, 1994): *Cooke* (1953) and *Green* (1970) fitted distributions of wet/dry precipitation spell durations using Markov chains; *Stern and Coe* (1984) described precipitation occurrences with a Markov chain defined by seasonal parameters; Markov chains were also used by *Haan et al.* (1976) to model precipitation as a process shifting between several states, each of them representing a precipitation amount interval; *Zucchini and Guttorp* (1991) modelled multi-gauge precipitation occurrences by assuming a different set of probabilities for each of a number of common unobservable climate states following a Markov chain; *Fortin et al.* (2004) applied a shifting level model, where a continuous Markovian process described mean runoff, to detect streamflow regime changes and forecast annual time series; *Akintuğ and Rasmussen* (2005) assumed the runoff probability distribution to be conditioned on a hidden climate state following a Markov chain, in order to generate synthetic time series of annual streamflow.

Precipitation downscaling originates from the desire to generate time series that are consistent with atmospheric information. Atmospheric variables can be predicted by the physically-based general circulation models (GCMs), which have been extensively used to generate climate change scenarios (*Hughes et al.*, 1993). Since

GCMs simulate atmospheric processes on very large grids, they are not suitable for predicting precipitation, which is characterised by high spatial variability (*Hughes and Guttorp*, 1994). Several studies, e.g. *Giorgi and Mearns* (1991) and *Bates et al.* (1998), indicated the need for downscaling approaches that could translate GCM simulations and historical records of large-scale atmospheric variables into local-scale precipitation. *Giorgi and Mearns* (1991) used a GCM to provide the boundary conditions for a nested limited area meteorological model, which simulated precipitation on a finer grid. However, this methodology implies high computational costs hindering its applicability. Moreover, biases of large-scale GCM simulations are likely to propagate to local-scale predictions (*Hughes et al.*, 1993; *Giorgi and Mearns*, 1991). Weather state models (WSMs) were first developed by *Hay et al.* (1991): WSMs downscale atmospheric information to local precipitation by classifying observed atmospheric patterns into weather types, which can be defined by either expert meteorological knowledge (*Bardossy and Plate*, 1991) or automatic classification methods (*Hughes et al.*, 1993); then precipitation probability distributions are estimated for each weather state. Non-homogeneous hidden Markov models (NHMMs) for precipitation were developed by *Hughes and Guttorp* (1994), *Hughes et al.* (1999), and *Bellone et al.* (2000). Unlike WSMs, NHMMs do not define the weather types by classifying atmospheric patterns a priori: each weather type is identified by a precipitation probability distribution and is represented by a state of a non-homogeneous Markov chain, whose state transition probabilities depend on atmospheric variables. Thus NHMMs define the weather states by considering both atmospheric and precipitation patterns. Such definition may yield more efficient models than WSMs, which identify the weather states without considering the precipitation process (*Charles et al.*, 1999). Recently NHMMs were applied by *Robertson et al.* (2004) to simulate precipitation occurrences in north-eastern Brazil, and by *Robertson et al.* (2007) to provide a crop model with precipitation input in south-eastern USA.

Several studies report of stochastic streamflow models using climatic information: *Uvo and Graham* (1998) applied canonical correlation analysis to perform seasonal streamflow forecasts in the Amazon Basin using Atlantic and Pacific Ocean sea surface temperature (SST); *Piechota and Dracup* (1999) combined autocorrelation and ENSO information to forecast streamflow in the Columbia river basin; *Kelman et al.* (2000) used ENSO data in an autoregressive model with exogenous input (ARX) to forecast aggregate streamflow in Colombia; *Landman et al.* (2001) applied statistical downscaling of GCM outputs to predict streamflow; *Grantz and*

Rajagopalan (2005) used regression methods to forecast streamflow from SST, snow water equivalent, and geopotential height. *Lu and Berliner* (1999) modelled daily streamflow with a Markov switching model (MSM): lagged streamflow and precipitation influenced state transition probabilities and were used in state-dependent linear regressions to predict streamflow.

1.1.2 Review of reservoir optimisation methods

Most existing reservoir operation policies are based on heuristic rules or subjective judgements of the operators. Thus many reservoir projects have not completely yielded the planned benefits (*WCD*, 2000). Furthermore, many policies are not designed for multi-facility systems, as integrated operational strategies dramatically increase the number of possible decisions (*Labadie*, 2004). Therefore the development of robust and feasible approaches to optimise reservoir operation has been extensively studied during the last decades (*Yeh*, 1985; *Simonovic*, 1992; *Wurbs*, 1993; *Labadie*, 2004). However a continuous gap between theoretical advances and real implementations has been observed. Mathematical complexity and difficulties in accounting for uncertainty of many optimisation methods were mentioned by *Labadie* (2004) among the causes of such gap. Considering input uncertainty is compulsory if inflow forecasts are exploited to improve operational efficiency. Input uncertainty in reservoir optimisation can be considered by either explicit (ESO) or implicit (ISO) stochastic optimisation methods (*Tickle and Goulter*, 1994). ESO integrates probabilistic descriptions of the input variables, thus directly accounting for uncertainty when optimising the policies. Instead, ISO evaluates operation policies on a number of equally likely input time series, thus indirectly including uncertainty. Theoretically, the operation policies obtained by applying ISO are valid only for the used input time series. However, compared to ESO, ISO allows a closer representation of the optimisation problem (*Karamouz and Houck*, 1987; *Rani and Moreira*, 2009) and yields lower computational costs in multireservoir applications (*Roefs and Bodin*, 1970).

Yeh (1985) and *Labadie* (2004) identified the main drawbacks of traditional optimisation algorithms, such as linear (LP) and dynamic (DP) programming, which can be implemented according to both ISO and ESO approaches: LP requires the system equations to be linear, when important processes such as hydropower generation are highly non-linear; DP is affected by the exponential growth of computational costs with the number of system state variables. Thus the applicability of these methods is often limited to simplified reservoir systems (*Chen*, 2003).

The simulation-optimisation (SO) approach, which belongs to the ISO framework, has been used to combine water resources simulation models with heuristics such as genetic algorithms (GAs). According to SO, optimisation is an iterative process in which trial solutions are first evaluated by the simulation model, and then used by the search algorithm to produce a new generation of trial solutions. Despite the high number of simulations required, SO has gained growing attention thanks to computational power advancements, its ease of implementation, and its applicability to non-linear and non-convex optimisation problems. GAs cannot guarantee the attainment of global optima, but can produce satisfactory solutions to problems where convergent algorithmic methods would lead to local optima or fail. Several authors have applied SO to water resources optimisation problems: *Oliveira and Loucks* (1997) used GAs to perform multi-objective optimisation of complex reservoir systems with constraints on releases and hydropower production; *Sharif and Wardlaw* (2000) used GAs to optimise a multi-reservoir system in the Brantas Basin in Indonesia; *Chen* (2003) combined a GA with a simulation model to optimise the rule curves of a reservoir system in Taiwan; *Ngo et al.* (2007) used the shuffled complex evolution algorithm to optimise the Hoa Binh reservoir in Vietnam. Several stochastic water resources optimisation problems were tackled by coupling GAs with sampling objective functions, which average multiple noisy evaluations, in order to implicitly account for input or parameter uncertainty (*Smalley and Minsker*, 2000; *Gopalakrishnan et al.*, 2001; *Kapelan et al.*, 2006; *Wu et al.*, 2006).

Many of the aforementioned methods have been applied to optimise real-time reservoir operation. Several authors indicated that real-time operation using forecasts may yield better results than reactive control (*Labadie et al.*, 1981; *Mishalani and Palmer*, 1988; *Georgakakos*, 1989). Several reservoir optimisation applications were implemented using short-term inflow forecasts without including long-term information (*Simonovic and Burn*, 1989; *Mujumdar and Ramesh*, 1997, 1998). However, since forecast models generally perform poorly for large lead times, real-time reservoir operation may be improved by integrating information from optimised long-term operation (*Yeh*, 1985; *Celeste et al.*, 2008).

1.2 Overview of the proposed methods

In the first research application we used NHMMs to downscale synoptic atmospheric patterns to daily precipitation amounts. The model was applied to 51 pre-

cipitation gauges in Denmark and southern Sweden. To obtain realistic simulations for dense networks of gauges, the spatial dependence structure of precipitation must be explicitly modelled (*Hughes et al.*, 1999; *Bellone et al.*, 2000). *Hughes et al.* (1999) used the autologistic model for multivariate binary data to account for spatial correlation of precipitation occurrences. However, to limit the number of parameters, inter-gauge correlations were modelled as functions of the distance and direction between gauges. To model the precipitation occurrence probability patterns for each weather state, we applied Chow-Liu trees (*Chow and Liu*, 1968; *Meila and Jordan*, 2000). Chow-Liu trees approximate multivariate discrete distributions with products of bivariate distributions, thus identifying preferential correlation patterns among precipitation gauges. Chow-Liu trees were embedded in NHMMs by *Kirshner et al.* (2004) for modelling multivariate precipitation occurrences in south-western Australia. Our model was used to simulate precipitation amounts conditioned on time series of atmospheric variables, and to analyse the correspondence between precipitation and atmospheric patterns defined by the weather states. Paper I reports on these applications.

In the second application we model seasonal inflow to the Daule Peripa and Baba reservoirs (Ecuador) using ENSO information. Our methodology derives from the work of *Hamilton* (1989), who modelled gross domestic product with a mixture of autoregressive models shifting between growth and recession phases according to a hidden Markov chain. We extended this approach by modelling state transitions with a non-stationary Markov chain, as defined for NHMMs by *Hughes and Guttorp* (1994). The presented model defines a hidden climate state following a non-stationary Markov chain, whose transition probabilities are functions of climatic information. The occurring climate state sets the ARX parameters for mapping inflow anomalies as functions of lagged inflow and current climatic indices. Thus the presented model is an MSM and not a hidden Markov model, in which observations are independent conditioned on the hidden states (*Cappè et al.*, 2005). Inflow anomalies are given a non-stationary description accounting for autocorrelation and climatic influence through pseudo-linear relations. Such description may be an advantage compared to stationary periodic autoregressive models (PARs) (*Salas*, 1993; *Hipel and McLeod*, 1994), which may also include climatic indices as exogenous input. Indeed non-linearities between streamflow and climatic variables and in autocorrelation may not by properly modelled by PARs due to their linearity. Model applications, which are described in papers II, III and IV, were: inflow simulation based on ENSO time series; inflow forecast-

ing conditioned on ENSO forecasts, which are available with 9 month lead time; and a retrospective analysis of historical records to infer about the correspondence between inflow regimes, model-defined climate states, and ENSO phases.

Finally we considered the optimisation of the Daule Peripa and Baba reservoirs, which serve hydropower plants and downstream water users. We followed the SO approach to perform long- and short-term stochastic reservoir optimisation. To account for input uncertainty and thus obtain robust reservoir operations, the developed MSM was used to generate the stochastic input to simulate the reservoirs. The optimisation was performed by minimising a sampling objective function measuring the hydropower deficit. Long-term optimisation was performed by calibrating rule curves, using synthetic inflow scenarios generated by conditioninng on long ENSO time series. Short-term optimisation was carried out by integrating ENSO-based inflow forecasts with seasonal storage targets, thus combining short-term climatic information and long-term optimal management guidance. Papers III and IV report on these applications.

1.3 Structure of the thesis

This thesis has the following structure: in chapter 2 we characterise the case studies; in chapter 3 we outline the applied methods; in chapter 4 we discuss the main results; in chapter 5 we summarise the achievements of the conducted research; in chapter 6 we provide a list of abbreviations and symbols.

2 Case studies

In this chapter we introduce the case studies by presenting study areas and data. Section 2.1 gives an overview of the meteorology of southern Scandinavia, and of the precipitation and atmospheric data used for the downscaling application in paper I. Section 2.2 presents the Daule Peripa and Baba reservoir system, and the inflow and ENSO data used in papers II, III, and IV.

2.1 Southern Scandinavia

The study area of the precipitation downscaling application consists of Denmark and southern Sweden (see Figure 2.1a).

2.1.1 Meteorology

The weather of southern Scandinavia is strongly influenced by the dominating wind direction (*DMI*, 1997). When the westerlies push low pressure systems from the northern Atlantic Ocean to Scandinavia, frontal precipitation occurs. This weather type usually persists for some days and sometimes for a few weeks. If low pressure does not affect Scandinavia, then high pressure weather prevails, bringing stable and dry conditions. Winds blow from east when there is a pressure gradient between Fennoscandia and the continent: air masses, heated and moisturised by the Baltic sea, may bring precipitation over the eastern part of the region. This weather type is very stable, but less frequent than the westerly regime. As eastern winds, southern winds blow from the continent. During summer, these air masses convey humidity, often provoking squalls or thunderstorms. Northern winds are the least frequent: due to the lee effect of the Norwegian mountains, the northern and eastern parts of the region are characterised by dry conditions, while precipitation may occur over the south-western part. North-eastern winds often bring precipitation over Denmark, as cold air masses from Sweden are heated and moisturised by the Kattegat.

2.1.2 Precipitation and atmospheric data

Daily precipitation and atmospheric data were available from 1981 to 2003. Only autumn-winter periods (November-February) were considered. Indeed the small-scale convective processes causing spring-summer precipitation can hardly be predicted by large-scale atmospheric patterns (*Linderson*, 2001). Precipitation data

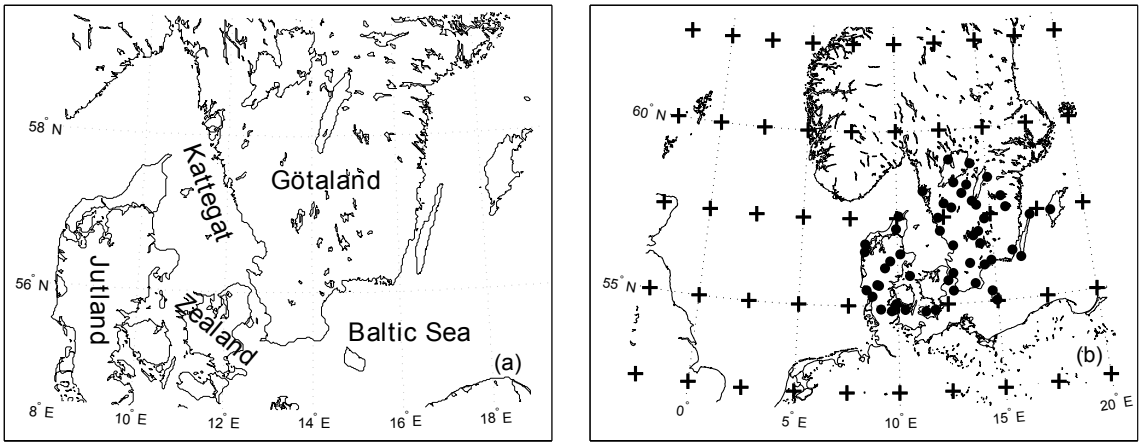

Figure 2.1: Overview of southern Scandinavia, precipitation gauges (·), and atmospheric grid nodes (+).

were obtained from the Danish Meteorological Institute (Copenhagen, Denmark) and the Swedish Meteorological and Hydrological Institute (Norrköping, Sweden) for 51 gauges (see Figure 2.1b). Time series of atmospheric variables were extracted from the NCEP Reanalysis dataset provided by the NOAA-CIRES Climate Diagnostics Center (Boulder, Colorado, USA). Among the available atmospheric fields, we chose geopotential height and relative humidity at several pressure levels because of their high relevance to precipitation: geopotential height informs on the circulation pattern, while relative humidity indicates the degree of saturation of the atmospheric layers. The variables are available on a grid with 2.5° resolution in latitude and longitude: the selected nodes are located in Figure 2.1b.

2.2 Western Ecuador

The hydrology of the coastal regions of Ecuador is strongly influenced by ENSO. ENSO can be characterised by standard indices based on SST anomalies (SSTA) of the equatorial Pacific Ocean (see Figure 2.2). ENSO is a cyclical phenomenon, in which El Niño and La Niña phases alternate with normal conditions.The expected duration of an El Niño or La Niña event is approximately 1 year, while return times normally range from 3 to 6 years. El Niño events can be defined as periods in which the 5 month moving average deviations of Niño 3 SST from the 1950-1979 monthly mean values are larger than +0.5°C for at least 6 consecutive months (*Trenberth*, 1997). A symmetric definition applies for La Niña, for which the upper threshold of smoothed SST deviations is -0.5°C. Occurrences of El Niño bring anomalously heavy precipitation in western Ecuador as a consequence of

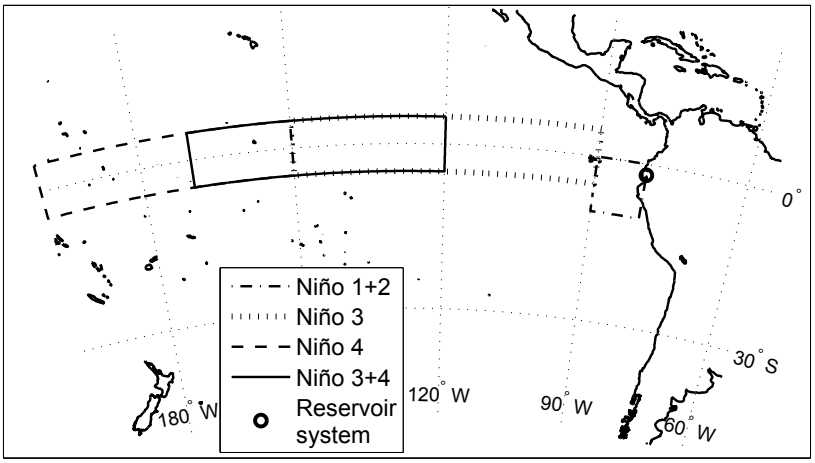

Figure 2.2: Location of the Daule Peripa and Baba reservoir system and parts of the Pacific Ocean where ENSO-related SST are measured.

positive SSTA along the coast (*Vuille et al.*, 1999). Moreover intense El Niño events may reverse the normal direction of trade winds, causing further increases in precipitation due to warm moist air masses moving from the Pacific Ocean to the coast.

2.2.1 Inflow and ENSO data

Monthly inflow data are available from 1950 to 2008 for Daule Peripa, and from 1950 to 2004 for Baba. The average inflow is 176 m^3/s for Daule Peripa, and 107 m^3/s for Baba. Approximately 92% of the difference concentrates between February and May, which constitute the wet season for both catchments (see Figure 2.3a). Indeed the average February-May inflow constitutes approximately 76% and 66% of the total annual inflow of Daule Peripa and Baba, respectively.

We analysed ENSO indices computed from SST measured on parts of the equatorial Pacific Ocean (see Figure 2.2): Niño 1+2 (0°-10°S, 90°-80°W), Niño 3 (5°N-5°S, 150°-90°W), Niño 3+4 (5°N-5°S, 170°-120°W), and Niño 4 (5°N-5°S, 160°E-150°W). We also considered the Trans-Niño Index (TNI), which is computed as the difference between Niño 1+2 and Niño 4 SSTA, thus representing the SSTA gradient across the equatorial Pacific Ocean (*Trenberth and Stepaniak*, 2001). Monthly SST data were obtained from the NOAA Climate Prediction Center[1] (Camp Springs, Maryland, USA) for 1950-2009. Monthly forecasts of ENSO-related SST are currently published with lead times up to 9 months.

[1] http://www.cpc.ncep.noaa.gov/data/indices/

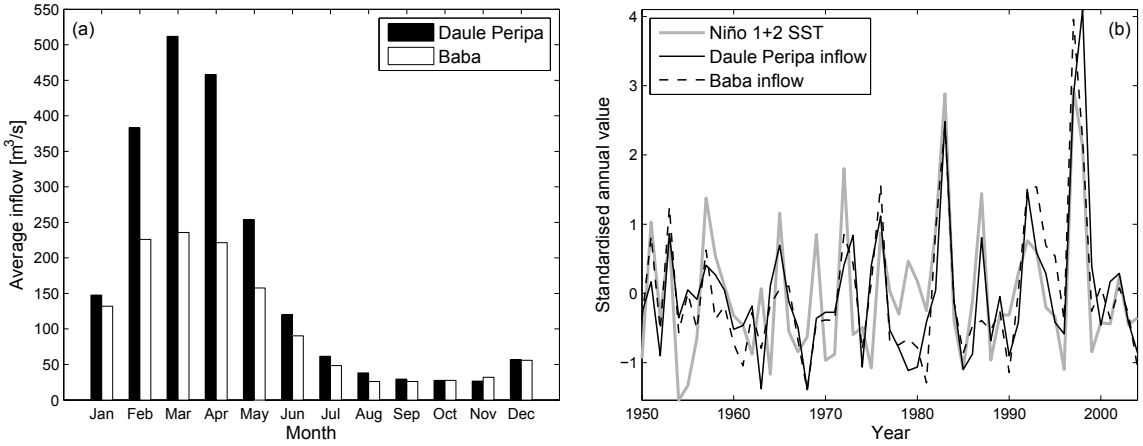

Figure 2.3: (a) Average monthly inflow of Daule Peripa and Baba reservoirs. (b) Annual time series of inflow anomalies and Niño 1+2 SSTA.

To give an overview of the correlation between ENSO indices and reservoir inflow, Figure 2.3b compares the annual anomalies of Niño 1+2 SST and inflow. Anomalies were obtained by standardising annual data with respect to sample mean and standard deviation. The annual inflow anomalies of Daule Peripa and Baba exhibit a significant cross-correlation. Niño 1+2 SSTA are well correlated with positive inflow anomalies, but not with anomalously low inflow. Similar results were obtained by comparing inflow anomalies with the other ENSO indices. This analysis suggested that El Niño is well correlated with positive inflow anomalies, while the influence of La Niña is not significant.

2.2.2 The Daule Peripa – Baba reservoir system

The approximate location of the studied reservoirs is shown in Figure 2.2. The Daule Peripa reservoir, which was completed in 1987, receives its inflow from the Daule and Peripa rivers. It serves a hydropower plant and other downstream water users. The Baba reservoir, currently under construction, will be supplied by the Baba river. It will serve downstream water users and a hydropower plant located along a transfer channel to Daule Peripa. The downstream water demands of both reservoirs are given highest priority and aggregate irrigation, urban water supply, and environmental flow demands.

The main characteristics and a scheme of the Daule Peripa – Baba water resources system are reported by Table 2.1 and Figure 2.4, respectively. The average annual inflow volume of Daule Peripa is 1.6 times its active storage volume. The same ratio scores 27 for Baba. Thus the water management potential of Baba is very lim-

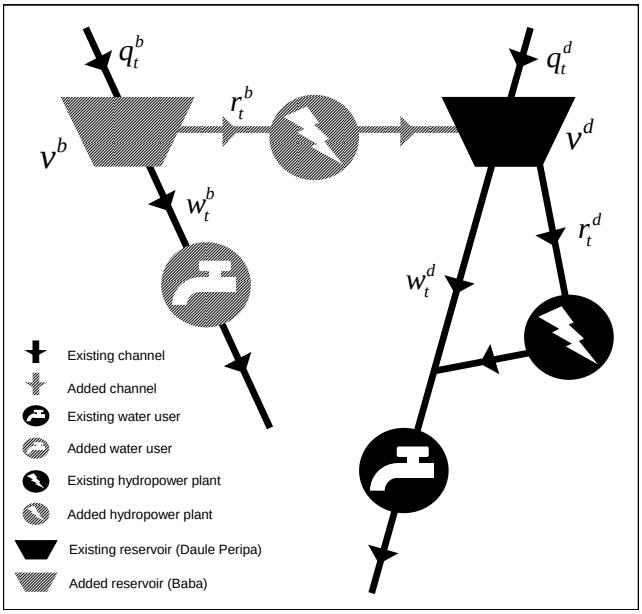

Figure 2.4: Scheme of the Daule Peripa – Baba water resources system: existing and added elements, and terms of the water balance equations (2.1) and (2.2).

Table 2.1: Characteristics of the Daule Peripa – Baba water resources system.

	Reservoir		Turbine			Downstream
	Active storage [km^3]	Level range [m]	Hydraulic capacity [m^3/s]	Power capacity [MW]	Average efficiency [-]	Water demand [m^3/s]
Daule Peripa	3.534	70-86	396	213	0.835	60
Baba	0.123	105-120	250	65	0.901	10

ited, compared to that of Daule Peripa. Indeed the inclusion of Baba will increase the total inflow by 60%, and the system storage capacity by only 3.5%. No defined operation policy is known for the existing or the planned water resources system. However, observed monthly time series of reservoir water level and hydropower are available from 2000 to 2008 for Daule Peripa.

Due to data scarcity, we defined the reservoir water balance and hydropower equations according to the following assumptions.

1. Inflows are net values, thus precipitation and evaporation at the lake surface, as well as storage gains and losses due to filtration, are not explicitly considered.

2. Time steps are monthly.

3. Water flows are constant during a time step.

Thus the water balance equations for time step t are

$$v^d(x) = v^d(\tau_{t-1}) + (x - \tau_{t-1})\left(q_t^d + r_t^b - r_t^d - w_t^d\right) \tag{2.1}$$

$$v^b(x) = v^b(\tau_{t-1}) + (x - \tau_{t-1})\left(q_t^b - r_t^b - w_t^b\right) \tag{2.2}$$

where τ_{t-1} is the end time of time step $t-1$; the superscript indices ^{d} and ^{b} refer to, respectively, Daule Peripa and Baba; $v^i(x)$ is the storage volume at time x, and q_t^i, r_t^i and w_t^i are inflow, turbine flow and downstream release during t, for $i = d, b$ and $\tau_{t-1} < x \leqslant \tau_t$. The terms of equations (2.1) and (2.2) are associated to the elements of the system in Figure 2.4. Let g_t be the average power generated by the hydropower plants during t:

$$g_t = \phi \sum_{i=d,b} \varepsilon^i r_t^i \left(\overline{h}_t^i - k_t^i\right) \tag{2.3}$$

where ϕ is the specific weight of water; ε^i is the turbine efficiency, and k_t^i and $\overline{h}_t^i$ are the tailwater height and the average reservoir water level during t, for $i = d, b$. Tailwater height and average reservoir level are non-linear functions of r_t^i, thus equation 2.3 is highly non-linear.

According to the water balance equations (2.1) and (2.2), system operation during t is defined by r_t^i and w_t^e, for $i = d, b$. However, to reduce the number of control variables, considering that downstream water demands prioritised, we made the following further assumptions. Let W^i be the downstream water demand, and R^i be the turbine hydraulic capacity, for $i = d, b$ (see Table 2.1):

4. $r_t^d \geqslant W^d$ unless the Daule Peripa reservoir is empty.

5. $w_t^b \geqslant W^b$ unless the Baba reservoir is empty.

6. $r_t^b > 0$ if and only if $w_t^b \geqslant W^b$.

7. $w_t^d = 0$ unless $r_t^d = R^d$ and the Daule Peripa reservoir is full.

8. $w_t^b > W^b$ if and only if $r_t^b = R^b$ and the Baba reservoir is full.

Assumptions 4, 5 and 6 derive from prioritising the downstream water demands. Assumption 7 takes into account that the turbine release of Daule Peripa is available to the downstream water users. Assumption 8 states that the downstream

release of Baba may exceed the water demand if and only if the Baba reservoir is full and the turbine hydraulic capacity is reached. According to all formulated assumptions, system operation during t is determined by the sole releases r_t^d and r_t^b. Let us define the system control variables during t as the turbine release fractions $\boldsymbol{\rho}_t = \left\{\rho_t^d, \rho_t^b\right\}$:

$$r_t^d = W^d + \rho_t^d \left(R^d - W^d\right) \tag{2.4}$$

$$r_t^b = \rho_t^b R^b \tag{2.5}$$

where $0 \leqslant \rho_t^i \leqslant 1$ so that $r_t^i \leqslant R^i$ (for $i = d, b$), and $r_t^d \geqslant W^d$.

3 Methods

In this chapter we summarise the applied methods. Section 3.1 describes the approaches to stochastic hydrologic modelling with climatic input used in papers I, II, III, and IV. The precipitation and inflow models are both based on the assumption that an unobservable state variable conditions the observable process. Thus section 3.1 first illustrates how the state is modelled, and then specifies the conditional descriptions of precipitation and inflow (in sections 3.1.1 and 3.1.2, respectively). Section 3.2 illustrates the reservoir optimisation methods applied in papers III and IV.

3.1 Stochastic hydrologic modelling with climatic input

The proposed stochastic models assume the observable hydrologic processes to be driven by a hidden climatic state. The state at time t is represented by the discrete stochastic variable s_t taking on values $1, \ldots, S$. s_t follows a first order Markov chain, whose transition probabilities depend on the climatic input at t. According to *Hughes and Guttorp* (1994), state transition probabilities can be computed as

$$\Pr\{s_t \,|s_{t-1}, \mathbf{c}_t, \boldsymbol{\theta}\} \propto p_{s_{t-1}s_t} \exp\left[-\frac{1}{2}\left(\mathbf{c}_t - \boldsymbol{\mu}_{s_t}\right)' \mathbf{V}^{-1}\left(\mathbf{c}_t - \boldsymbol{\mu}_{s_t}\right)\right], \text{ if } t > 1 \quad (3.1)$$

where $\mathbf{c}_t$ is the vector of climatic indices at t; $\boldsymbol{\theta}$ is the model parameters set; p_{ij} is the stationary component of the transition probability from state i to j; $\boldsymbol{\mu}_i$ is the value of $\mathbf{c}_t$ that maximises the probability of shifting to state i; and $'$ is the transpose operator; to limit parameter numerosity, the scale matrix $\mathbf{V}$ is set equal to the covariance matrix of $\mathbf{c}_t$ (*Hughes and Guttorp*, 1994; *Hughes et al.*, 1999; *Bellone et al.*, 2000). To ensure parameter identifiability, p_{ij} is subject to the constraint $\sum_{j=1}^{S} p_{ij} = 1$, for $i = 1, \ldots, S$. State occurrence probabilities for the first time step are calculated as

$$\Pr\{s_1 \,|\mathbf{c}_1, \boldsymbol{\theta}\} \propto \exp\left[-\frac{1}{2}\left(\mathbf{c}_1 - \boldsymbol{\mu}_{s_1}\right)' \mathbf{V}^{-1}\left(\mathbf{c}_1 - \boldsymbol{\mu}_{s_1}\right)\right] \quad (3.2)$$

Let $\mathbf{a}_t$ and $\boldsymbol{\beta}_t$ be the vectors of, respectively, observable and conditioning variables at t. The content of $\boldsymbol{\beta}_t$ is specified in sections 3.1.1 and 3.1.2 for each modelling application. However, in the developed models, $\boldsymbol{\beta}_t$ may only consist of current and lagged (with respect to t) observable variables and climatic indices. Let $f_{\mathbf{a}}(\mathbf{a}_t \,|s_t, \boldsymbol{\beta}_t, \boldsymbol{\theta})$ be the conditional probability density function (CPDF) of the

observable variables $\mathbf{a}_t$, given the state s_t, the conditioning variables $\boldsymbol{\beta}_t$, and the model parameters $\boldsymbol{\theta}$. Then, according to *MacDonald and Zucchini* (1997), the model likelihood function is

$$L\left(\boldsymbol{\theta}\,|\mathbf{a}_{1:T}, \mathbf{c}_{1:T}\right) = \boldsymbol{\psi}_1' \left(\prod_{t=2}^{T} \boldsymbol{\Psi}_t\right) \mathbf{1}_S \tag{3.3}$$

where T is the last time step of the series; $\mathbf{a}_{1:T}$ and $\mathbf{c}_{1:T}$ are the time series of, respectively, $\mathbf{a}_t$ and $\mathbf{c}_t$ from time step 1 to T; $\mathbf{1}_{(S)}$ is a S long vector of ones; and the elements of the S long vector $\boldsymbol{\psi}_1$ and of the $S \times S$ matrix $\boldsymbol{\Psi}_t$ are

$$\psi_1\left(s_1\right) = f_{\mathbf{a}}\left(\mathbf{a}_1\,|s_1, \boldsymbol{\beta}_1, \boldsymbol{\theta}\right) \Pr\left[s_1\,|\mathbf{c}_1, \boldsymbol{\theta}\right] \tag{3.4}$$

$$\Psi_t\left(s_{t-1}, s_t\right) = f_{\mathbf{a}}\left(\mathbf{a}_t\,|s_t, \boldsymbol{\beta}_t, \boldsymbol{\theta}\right) \Pr\left[s_t\,|s_{t-1}, \mathbf{c}_t, \boldsymbol{\theta}\right], \text{ if } t > 1 \tag{3.5}$$

Model parameters $\boldsymbol{\theta}$ are estimated by maximising the likelihood function (3.3) with the expectation-maximisation (EM) algorithm. The EM algorithm, which is an iterative maximum likelihood method, was originally developed for hidden Markov models (*Baum et al.*, 1970; *Dempster et al.*, 1977), and later applied to NHMMs by *Hughes et al.* (1999). Paper I outlines the EM algorithm for NHMMs, while for MSMs full derivations are carried out in the appendices of papers III and IV.

The presented general modelling framework can be used for simulation, forecasting, and retrospective analysis of historical records. By simulating, we generate a set of synthetic time series of observable variables $\widehat{\mathbf{A}}_{1:T}^{N} = \left\{\widehat{\mathbf{a}}_{1:T}^{(1)}, \ldots, \widehat{\mathbf{a}}_{1:T}^{(N)}\right\}$, given a time series of climatic variables $\mathbf{c}_{1:T}$. Forecasting for lead times up to l (from the end of time step t) is done by generating $\widehat{\mathbf{A}}_{t+1:t+l}^{N}$ conditioned on past observations $\mathbf{a}_{1:t}$ and $\mathbf{c}_{1:t}$, and on climatic forecasts $\widehat{\mathbf{c}}_{t+1:t+l}$. Retrospective analysis of historical records is carried out via the Viterbi algorithm (*Viterbi*, 1967; *Rabiner*, 1989), which finds the most likely state sequence $\mathbf{s}_{1:T}^{*} = \{s_1^{*}, \ldots, s_T^{*}\}$ given the observed time series $\mathbf{a}_{1:T}$ and $\mathbf{c}_{1:T}$:

$$\mathbf{s}_{1:T}^{*} = \underset{\mathbf{s}_{1:T}}{\arg\max} \left\{\Pr\left[\mathbf{s}_{1:T}\,|\mathbf{a}_{1:T}, \mathbf{c}_{1:T}, \boldsymbol{\theta}\right]\right\} \tag{3.6}$$

Simulation, forecasting, and retrospective analysis techniques are described in papers I, II, and IV.

3.1.1 Downscaling atmospheric patterns to precipitation

In the precipitation modelling application, the observable variables $\mathbf{a}_t$ are the precipitation amounts observed at K gauges on day t. The hidden state variable s_t is

referred to as the weather state. The climatic inputs $\mathbf{c}_t$ are atmospheric summary variables obtained by applying singular value decomposition (SVD) to the gridded atmospheric fields. SVD reduces the high dimensional atmospheric data into a few values that explain most of the covariance between the atmospheric fields and precipitation (*Bretherton et al.*, 1992). The SVD technique is described in paper I.

We assume that precipitation is conditioned only on the current weather state and model parameters, according to the definition of hidden Markov model (*Cappè et al.*, 2005). Thus the CPDF of $\mathbf{a}_t$ is

$$f_{\mathbf{a}}\left(\mathbf{a}_t \left| s_t, \boldsymbol{\theta}\right.\right) = f_{\boldsymbol{\alpha}}\left(\boldsymbol{\alpha}_t \left| s_t, \boldsymbol{\theta}\right.\right) \prod_{k=1}^{K} \mathrm{Ga}\left(a_t\left(k\right) - e; \xi_{ks_t}, \varphi_{ks_t}\right)^{\alpha_t(k)} \tag{3.7}$$

where $a_t\left(k\right)$ is the precipitation amount at gauge k on day t; e is the typical resolution of a tipping bucket rain gauge (0.2 mm); $\mathrm{Ga}\left(\cdot\,; \xi_{ki}, \varphi_{ki}\right)$ is a two parameter Gamma density with parameters ξ_{ki} and φ_{ki}, which are specific for gauge k when state i occurs; $\boldsymbol{\alpha}_t$ is the precipitation occurrence pattern on day t: if precipitation occurs at gauge k, then $\alpha_t\left(k\right) = 1$, otherwise $\alpha_t\left(k\right) = 0$; $f_{\boldsymbol{\alpha}}\left(\boldsymbol{\alpha}_t \left| s_t, \boldsymbol{\theta}\right.\right)$ is the conditional probability mass function (CPMF) of $\boldsymbol{\alpha}_t$, given s_t. If we assume that precipitation occurrences at different gauges are conditionally independent given the weather state, the CPMF of $\boldsymbol{\alpha}_t$ becomes

$$f_{\boldsymbol{\alpha}}^{I}\left(\boldsymbol{\alpha}_t \left| s_t, \boldsymbol{\theta}\right.\right) = \prod_{k=1}^{K} \left(o_{ks_t}\right)^{\alpha_t(k)} \left(1 - o_{ks_t}\right)^{1-\alpha_t(k)} \tag{3.8}$$

where o_{ki} is the precipitation occurrence probability at gauge k for state i. However, the description given in equation (3.8), in which the spatial correlation of precipitation is implicitly accounted for by the weather state, is not suitable for dense gauge networks (*Hughes et al.*, 1999; *Bellone et al.*, 2000).

To explicitly model the spatial dependence of precipitation occurrences, NHMMs can be combined with Chow-Liu trees for multivariate discrete data (*Chow and Liu*, 1968; *Meila and Jordan*, 2000; *Kirshner et al.*, 2004). The Chow-Liu method approximates a multivariate distribution of K discrete variables with the product of $K - 1$ bivariate discrete distributions. Such pairs constitute the tree structure, in which the edges are not allowed to form circles. Let E_i be the Chow-Liu tree for

state i, the tree-approximated CPMF of $\boldsymbol{\alpha}_t$ becomes

$$f_{\boldsymbol{\alpha}}^{T}\left(\boldsymbol{\alpha}_t \left| s_t, \boldsymbol{\theta}\right.\right) = \frac{\prod_{(k,j)\in E_{s_t}} F_{kj}\left(\alpha_t\left(k\right), \alpha_t\left(j\right) \left| s_t, \boldsymbol{\theta}\right.\right)}{\prod_{k=1}^{K} F_k\left(\alpha_t\left(k\right) \left| s_t, \boldsymbol{\theta}\right.\right)^{\deg(k)-1}} \tag{3.9}$$

where $F_{kj}\left(\alpha_t\left(k\right), \alpha_t\left(j\right) \left| s_t, \boldsymbol{\theta}\right.\right)$ is the conditional bivariate discrete distribution of precipitation occurrences at gauges k and j; $F_k\left(\alpha_t\left(k\right) \left| s_t, \boldsymbol{\theta}\right.\right)$ is the marginal of $F_{kj}\left(\alpha_t\left(k\right), \alpha_t\left(j\right) \left| s_t, \boldsymbol{\theta}\right.\right)$ with respect to $\alpha_t\left(j\right)$ for any $j \neq k$; $\deg\left(k\right)$ is the number of tree edges connecting gauge k. At each iteration of the model calibration procedure, the tree edges are selected by maximising the total conditional mutual information, which measures the amount of explained covariance between pairs of discrete variables (see paper I for details). Thus the tree E_i identifies a preferential correlation pattern among precipitation gauges for state i. The number of parameters needed by the Chow-Liu tree approximation increases linearly with the number of gauges K, while a multivariate discrete distribution yields an exponential increase (*Hughes and Guttorp*, 1994).

3.1.2 Inflow modelling using ENSO information

In the inflow modelling application, $\mathbf{a}_t$ and $\mathbf{c}_t$ are monthly anomalies of reservoir inflow and ENSO indices, respectively. Inflow anomalies are obtained by log-transformation and deseasonalisation, while ENSO indices are only deseasonalised (see paper II) II. Here, the hidden state variable s_t is referred to as the climate state. The climate state determines the parameters of the multivariate ARX modelling inflow anomalies. Assuming the conditional multivariate ARX noise to consist of Gaussian stationary white noise uncorrelated processes, the CPDF of $\mathbf{a}_t$ is

$$f_{\mathbf{a}}\left(\mathbf{a}_t \left| s_t, \mathbf{a}_{t-1}, \mathbf{c}_t, \boldsymbol{\theta}\right.\right) = \frac{1}{\sqrt{\left(2\pi\right)^{K} \det\left(\boldsymbol{\Omega}_{s_t}\right)}}$$
$$\exp\left[\frac{1}{2}\left(\mathbf{a}_t - \boldsymbol{\delta}_{s_t} - \mathbf{D}_{t-1}\boldsymbol{\lambda}_{s_t} - \boldsymbol{\Gamma}_{s_t}\mathbf{c}_t\right)' \boldsymbol{\Omega}_{s_t}^{-1}\left(\mathbf{a}_t - \boldsymbol{\delta}_{s_t} - \mathbf{D}_{t-1}\boldsymbol{\lambda}_{s_t} - \boldsymbol{\Gamma}_{s_t}\mathbf{c}_t\right)\right] \tag{3.10}$$

where $\mathbf{a}_0$ is defined to be a null vector; K is the number of inflow gauges; $\mathbf{D}_t$ is a diagonal matrix constituted by the elements of $\mathbf{a}_t$; $\boldsymbol{\delta}_i$, $\boldsymbol{\lambda}_i$, $\boldsymbol{\Gamma}_i$, and $\boldsymbol{\Omega}_i$ are the multivariate ARX parameters for state i. In particular, $\boldsymbol{\delta}_i$ is the K long vector of intercept parameters; $\boldsymbol{\lambda}_i$ is the K long vector of autoregressive parameters; $\boldsymbol{\Gamma}_i$ is the $K \times M$ matrix of exogenous correlation parameters, where M is the length of $\mathbf{c}_t$; and $\boldsymbol{\Omega}_i$ is the $K \times M$ covariance matrix of the multivariate residual process:

$$\boldsymbol{\Omega}_i = \operatorname{cov}\left\{\mathbf{a}_t - \boldsymbol{\delta}_i - \mathbf{D}_{t-1}\boldsymbol{\lambda}_i - \boldsymbol{\Gamma}_i\mathbf{c}_t\right\} = \boldsymbol{\Xi}_i\boldsymbol{\phi}_i\boldsymbol{\Xi}_i', \text{ if } s_t = i \tag{3.11}$$

where the columns of Ξ_i are the eigenvectors of Ω_i; and the elements of the diagonal matrix $\boldsymbol{\phi}_i$ are the eigenvalues of Ω_i. Thus the conditional description of $\mathbf{a}_t$ is

$$\mathbf{a}_t = \boldsymbol{\delta}_i + \mathbf{D}_{t-1}\boldsymbol{\lambda}_i + \boldsymbol{\Gamma}_i\mathbf{c}_t + \boldsymbol{\Xi}_i\boldsymbol{\phi}_i^{\frac{1}{2}}\boldsymbol{\varepsilon}_t, \text{ if } s_t = i \tag{3.12}$$

where $\boldsymbol{\varepsilon}_t$ is a vector of standard Gaussian independent white noise processes.

The proposed approach mimics discrete climate-driven inflow regime shifts, and directly models correlations between ENSO indices and inflow anomalies. Since the multivariate ARX parameters are determined by the climate state, inflow anomalies are given a heteroschedastic and pseudo-linear description.

3.2 Reservoir optimisation methods

The presented reservoir optimisation methods are designed to exploit the ability of the inflow model defined in 3.1.2 to generate inflow scenarios consistently with the available ENSO information. Optimisation is carried out according to the SO approach by coupling the reservoir system simulation model defined in section 2.2.2 with a GA.

GAs are heuristics designed to find approximate solutions to search and optimisation problems (*Goldberg*, 1989; *Holland*, 1992). The operation of a GA consists of the following steps: (i) an initial population of solutions is randomly generated; (ii) objective functions are evaluated for each member of the initial population; (iii) a new population is generated by the genetic operators (selection, crossover and mutation); (iv) steps (ii) and (iii) are iterated until a termination criterion is satisfied.

According to the assumptions made in section 2.2.2, the downstream water demands of the Daule Peripa and Baba reservoirs are given highest priority. Thus reservoir optimisation is defined as a single-objective problem, in which the minimisation of the expected root mean square hydropower deficit (ERMSHD) is sought. Input uncertainty is accounted by using sampling objective functions that evaluate each trial set of decision variables on a high number of synthetic inflow time series. The number of used synthetic time series is decided by compromising between the following conflicting criteria: (i) if simulations are iterated on several sets of time series, a set of decision variables must yield similar objective function values (stability criterion); (ii) the computational cost of the stochastic evaluation

must be acceptable (feasibility criterion).

Section 3.2.1 defines the long-term optimisation technique (LT), which uses simulated inflow scenarios based on long time series of ENSO indices as stochastic input. Section 3.2.2 defines the short-term optimisation technique (ST), which optimises reservoir releases at each monthly time step using ENSO-based inflow forecasts issued for the following 9 months. To benchmark the performance of the optimisation methods, we apply the DP algorithm (*Bellman*, 1957; *Bertsekas*, 2000): given a finite set of reservoir water levels and assuming perfect knowledge of inflow, the DP algorithm finds the water level time series minimising ERMSHD while fulfilling the downstream water demands. The optimisation problems solved by the DP algorithm are defined in papers III and IV.

3.2.1 Long-term optimisation

LT optimises rule curves that determine reservoir releases as functions of reservoir water levels and calendar month. A rule curve consists of 12 reservoir water levels, one per calendar month, which are the upper bounds for the implementation of a pre-defined release fraction.

Let $\boldsymbol{\eta}_u^k = \left\{\eta_u^k(1), \ldots, \eta_u^k(12)\right\}$ be the uth rule curve for reservoir k, and υ_u^k be the corresponding pre-defined release fraction. Let $h^k(x)$ be the water level of reservoir k at time x, and $\rho^k(x)$ be the corresponding actual release fraction. During the monthly time step t, i.e. when $\tau_{t-1} < x \leqslant \tau_t$, we have that

$$\eta_{u+1}^k(m(t)) < h^k(x) \leqslant \eta_u^k(m(t)) \Rightarrow \rho^k(x) = \upsilon_u^k \tag{3.13}$$

where $m(t)$ returns the calendar month corresponding to t; the rule curves are defined so that $\eta_u^k(z) < \eta_{u-1}^k(z)$, and $\upsilon_{u-1}^k < \upsilon_u^k$. Two additional fixed rule curves are needed for each reservoir to fulfil the reservoir water level constraints:

$$\boldsymbol{\eta}_0^k = h_{max}^k \mathbf{1}_{(12)} \tag{3.14}$$

$$\boldsymbol{\eta}_{U+1}^k = h_{min}^k \mathbf{1}_{(12)} \tag{3.15}$$

corresponding to $\upsilon_0^k = 1$ and $\upsilon_{U+1}^k = 0$, where h_{min}^k and h_{max}^k are the minimum and maximum operational water levels of reservoir k (see Table 2.1), and $\mathbf{1}_{(12)}$ is a 12 long vector of ones. The average release fraction of reservoir k during t, i.e. ρ_t^k, is then computed as the average of $\rho^k(x)$ for $\tau_{t-1} < x \leqslant \tau_t$.

If U rule curves have to be optimised, to limit the number of variables to be optimised, only $\boldsymbol{\eta}_1^k$ is defined by 12 levels, whereas the other $U-1$ rule curves are

defined by scaling factors:

$$\boldsymbol{\eta}_u^k = h_{min}^k \mathbf{1}_{(12)} + \chi_{u-1}^k \left(\boldsymbol{\eta}_{u-1}^k - h_{min}^k \mathbf{1}_{(12)} \right), \text{ for } u = 2, \ldots, U \tag{3.16}$$

where χ_{u-1}^k is the scaling factor defining the uth rule curve of reservoir k. For each reservoir k, the set of decision variables is $\left\{ \boldsymbol{\eta}_1^k, \chi_1^k, \ldots, \chi_{U-1}^k \right\}$. Thus the total number of variables to be optimised is $K\,(U + 11)$. The presented rule curve parameterisation imitates traditional reservoir operation, in which releases are often determined as functions of reservoir water level and season (*Wurbs*, 1993).

Let $\mathbf{H}_{LT}$ be the complete set of LT decision variables; $\widehat{\mathbf{Q}}_{1:T}^N = \left\{ \widehat{\mathbf{q}}_{1:T}^{(1)}, \ldots, \widehat{\mathbf{q}}_{1:T}^{(N)} \right\}$ be a set of N synthetic reservoir inflow time series from month 1 to T; and $\widehat{\mathbf{R}}_{1:T}^N = \left\{ \widehat{\mathbf{r}}_{1:T}^{(1)}, \ldots, \widehat{\mathbf{r}}_{1:T}^{(N)} \right\}$ and $\widehat{\mathbf{g}}_{1:T}^N = \left\{ \widehat{g}_{1:T}^{(1)}, \ldots, \widehat{g}_{1:T}^{(N)} \right\}$ be the corresponding sets of releases and hydropower time series obtained by simulating the water resources system implementing $\mathbf{H}_{LT}$, given $\widehat{\mathbf{Q}}_{1:T}^N$. Assuming the sum of the turbine power capacities to be the power demand G (see Table 2.1), the sampling objective function estimating ERMSHD is

$$y\left(\widetilde{\mathbf{Q}}_{1:T}^N, \mathbf{H}_{LT} \right) = \sqrt{\frac{1}{NT} \sum_{n=1}^{N} \sum_{t=1}^{T} \left(G - \widehat{g}_t^{(n)} \right)^2} \tag{3.17}$$

3.2.2 Short-term optimisation

At the beginning of each monthly time step t, ST optimises reservoir operation according to the following procedure: (i) based on the available 9 month long forecasts of ENSO indices $\widehat{\mathbf{c}}_{t:t+8}$, a set of inflow forecast scenarios $\widehat{\mathbf{Q}}_{t:t+8}^N$ are generated by the stochastic inflow model described in section 3.1.2; (ii) the reservoir release fractions for the 9 month forecast period $\boldsymbol{\rho}_{t:t+8} = \left\{ \boldsymbol{\rho}_t, \ldots, \boldsymbol{\rho}_{t+8} \right\}$ are optimised using the inflow forecast scenarios as stochastic input; (iii) the system is operated during the first time step t by implementing the optimised value of $\boldsymbol{\rho}_t$; (iv) the reservoir water levels are updated at the end of t; (v) steps from (i) to (iv) are iterated for $t + 1$.

At the beginning of t, $\boldsymbol{\rho}_{t:t+8}$ are optimised by minimising an aggregate objective function, which is a weighted sum of ERMSHD from t to $t + 8$ and of a penalty

term approximating the minimum ERMSHD beyond the forecast horizon:

$$Y\left(\widehat{\mathbf{Q}}_{t:t+8}^{N}, \boldsymbol{\rho}_{t:t+8}\right) = (1-\omega)\sqrt{\frac{1}{9N}\sum_{n=1}^{N}\sum_{l=0}^{8}\left(G-\widehat{g}_{t+l}^{(n)}\right)^{2}} + \frac{\omega}{N}\sum_{n=1}^{N}P\left(m\left(t+8\right), \widehat{\mathbf{h}}_{t+8}^{(n)}\right) \quad (3.18)$$

where $\widehat{\mathbf{h}}_{t+8}^{(n)} = \left\{\widehat{h}^{d(n)}\left(\tau_{t+8}\right), \widehat{h}^{b(n)}\left(\tau_{t+8}\right)\right\}$ is the vector of reservoir water levels at the end of $t+8$, obtained by implementing $\boldsymbol{\rho}_{t:t+8}$ given $\widehat{\mathbf{q}}_{t:t+8}^{(n)}$; $P\left(m\left(t+8\right), \mathbf{h}_{t+8}\right)$ is the penalty term as function of the calendar month and reservoir water levels at the end of the forecast period; and ω is the weight assigned to the penalty term ($0 \leqslant \omega \leqslant 1$).

To compute $P\left(m\left(t+8\right), \mathbf{h}_{t+8}\right)$, we sample a set of observed 12 month inflow time series beginning on calendar month $m\left(t+9\right)$. Given a finite set of feasible monthly reservoir water levels, constraining initial and final levels to be equal, and imposing the satisfaction of downstream water demands, the approximated minimum root mean square hydropower deficit (MRMSHD) for a single time series is found via the DP algorithm. The penalty term is computed by averaging the RMSHDs obtained for the single inflow time series. This definition of the penalty function yields the following properties: (i) the reservoir water levels minimising the penalty function can be interpreted as monthly storage targets; (ii) RMSHDs computed on the same inflow time series are based on the same cumulated reservoir releases; (iii) the stochasticity of inflow is accounted for by averaging single MRMSHD values. A detailed discussion of the penalty function is available in paper IV.

ST exploits both short- and long-term information to optimise reservoir operation at the beginning of every monthly time step. Short-term information consists of the 9 month long ENSO-based inflow forecasts. Long-term information is accounted for by the penalty function, which penalises deviations from monthly storage targets.

4 Results and discussion

In this chapter, we summarise and discuss the main results obtained during the PhD studies: section 4.1 presents the application of the stochastic precipitation model in southern Scandinavia; section 4.2 reports on the application of the stochastic inflow model to the Daule Peripa reservoir; section 4.3 compares LT and ST with the historical management of the Daule Peripa reservoir, and then illustrates the application of ST to the planned Daule Peripa – Baba water resources system. Although the methods described in sections 3.1.2 and 3.2 are defined for the two reservoir system, several results are available only for Daule Peripa. Indeed the inclusion of Baba needs to be further developed, by working on both the multivariate inflow model and the multi-reservoir optimisation methods.

4.1 Downscaling atmospheric patterns to precipitation in southern Scandinavia

NHMMs embedding Chow-Liu trees (see section 3.1.1) were calibrated on daily winter precipitation data recorded by 51 gauges in Denmark and Götaland (see Figure 2.1). We selected a NHMM defining 8 weather states and downscaling geopotential height at 1000 hPa (GH-1000) and relative humidity at 850 hPa. The fitted model yielded satisfactory reproductions of average precipitation amounts, and of gauge-specific statistics such as precipitation marginal distributions and wet- and dry-spell duration curves. A detailed discussion of these results is available in paper I. Here we illustrate the reproduction of the spatial correlation of precipitation, and the physical interpretation of the weather states.

Figure 4.1 compares the reproduction of the observed cross-correlation coefficients between precipitation amounts at pairs of gauges. The NHMM assuming conditional spatial independence systematically underestimates high correlations. The use of Chow-Liu trees yields a slightly better reproduction of large correlations. However underestimation remains systematic. Indeed Chow-Liu trees account for the spatial dependence of the precipitation occurrence process, but assume precipitation amounts at different gauges to be conditionally independent. Thus further improvement might be achieved by introducing a spatial dependence model for precipitation amounts.

The model-defined weather states can be associated to expected atmospheric pat-

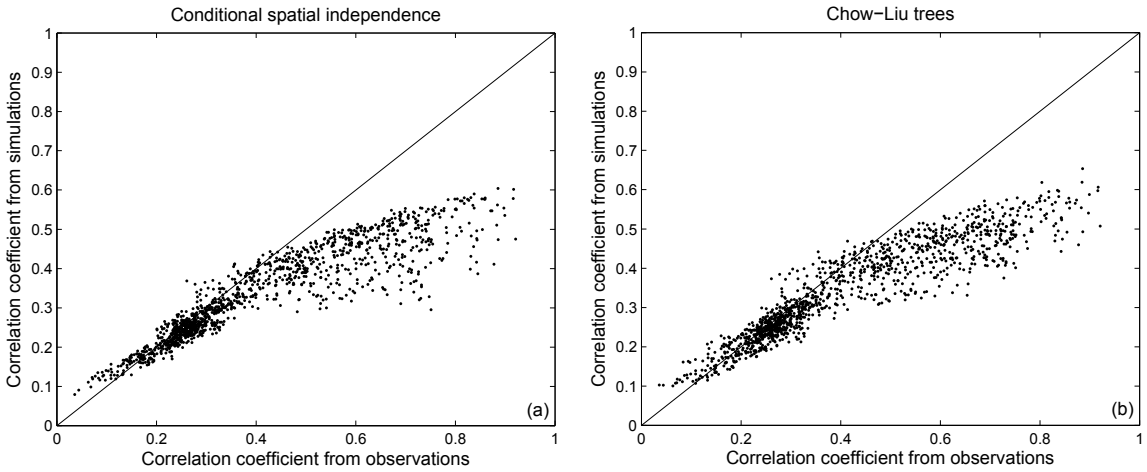

Figure 4.1: Observed correlation coefficients between precipitation at pairs of gauges versus values simulated with (a) conditional spatial independence, and (b) Chow-Liu trees.

terns, which are obtained by averaging the atmospheric time series using inferred state occurrences or occurrence probabilities as weights. The latter can be estimated via, respectively, Viterbi (*Viterbi*, 1967; *Rabiner*, 1989) and Baum-Welch (*Baum et al.*, 1970) algorithms, which are described in paper I. Comparing the state-specific precipitation probability distributions with the corresponding averaged atmospheric patterns allows validating the physical significance of the model. Here each weather state is characterised by the marginal precipitation occurrence probability pattern, the Chow-Liu tree, and the associated averaged pattern of GH-1000. A more complete discussion of the weather states, including expected precipitation amounts, is available in paper I.

State 1 corresponds to a high pressure weather type and yields small precipitation occurrence probabilities at all gauges (see Figure 4.2).

State 2 represents an intense westerly regime, in which a deep low pressure system approaches Scandinavia from the Norwegian Sea and causes winds to blow from the south-west. Consistently, precipitation probabilities are large at all gauges (see Figure 4.3).

State 3 corresponds to a weak westerly weather type, in which winds blow from the north-west. Precipitation probabilities are large in Denmark and low in Götaland, probably due to the lee effect of the Norwegian mountains (see Figure 4.4).

State 4 may correspond to the early development of a low pressure area causing

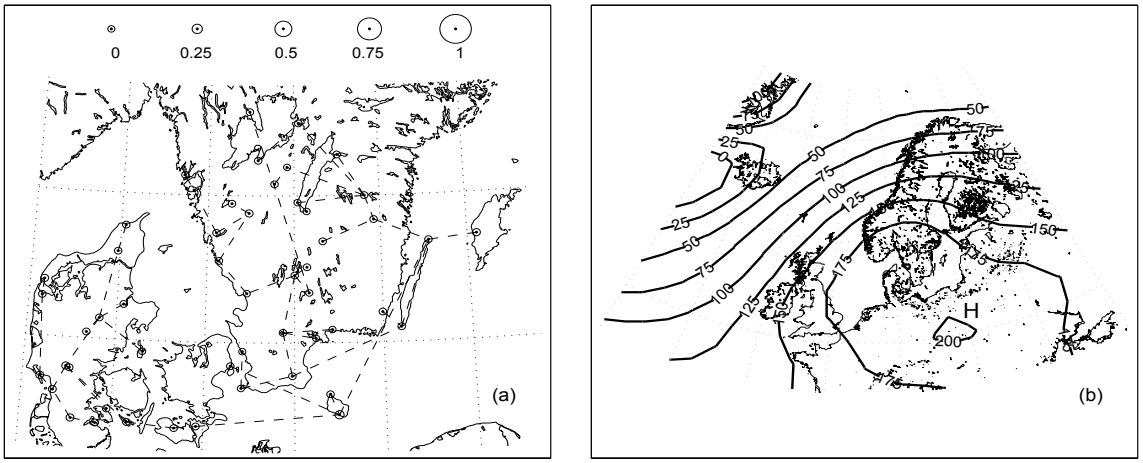

Figure 4.2: Weather state 1: (a) precipitation occurrence probabilities and edges of the Chow-Liu tree; (b) averaged GH-1000 pattern.

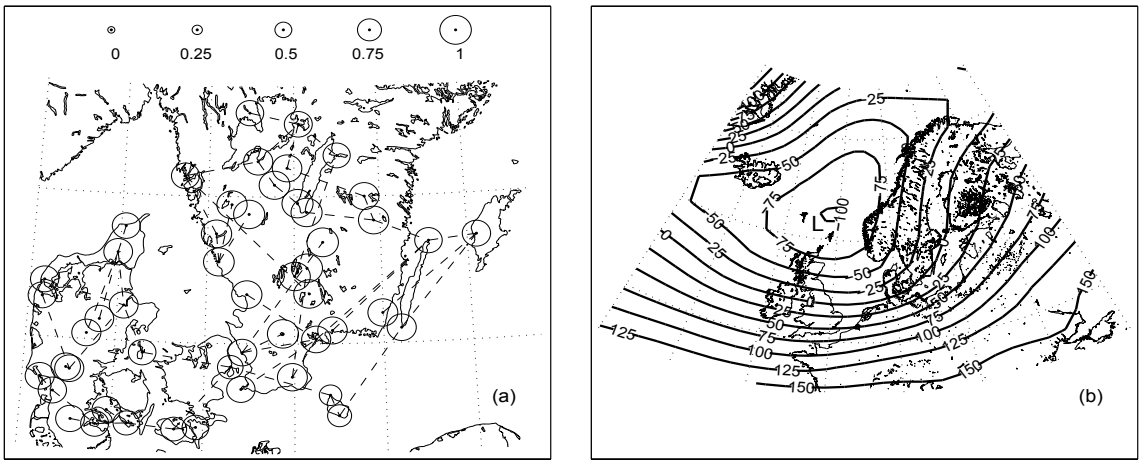

Figure 4.3: Weather state 2: (a) precipitation occurrence probabilities and edges of the Chow-Liu tree; (b) averaged GH-1000 pattern.

weak westerly conditions. Precipitation probabilities are larger in Götaland than in Denmark, possibly because of air masses being heated and moisturised by the Kattegat (see Figure 4.5).

State 5 is similar to state 4, corresponding to an even less developed low pressure system. Consistently, precipitation probabilities for state 5 are smaller than for state 4 at all gauges (see Figure 4.6).

State 6 corresponds to an easterly weather type, characterised by high pressure on Russia and Fennoscandia. Consistently, precipitation probabilities are highest in the easternmost part of the study area and gradually decrease westwards (see

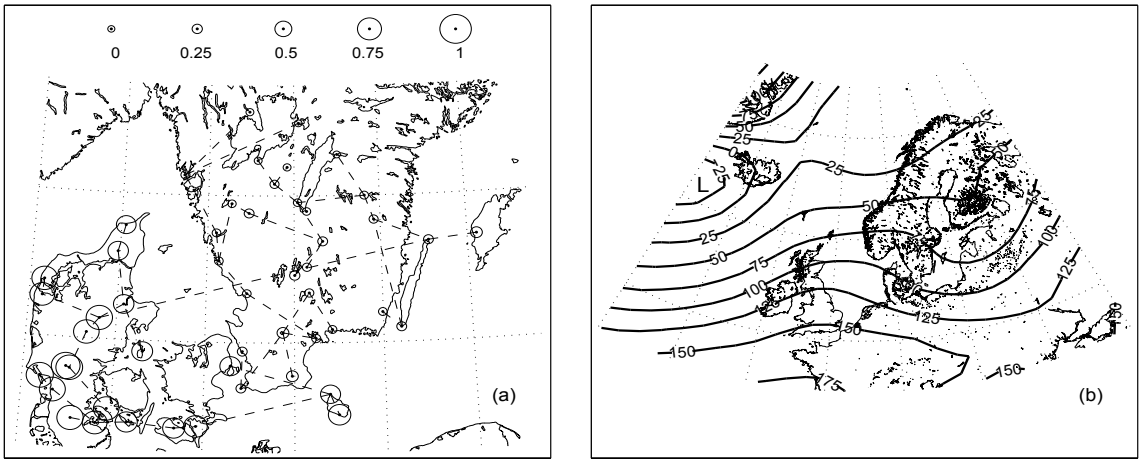

Figure 4.4: Weather state 3: (a) precipitation occurrence probabilities and edges of the Chow-Liu tree; (b) averaged GH-1000 pattern.

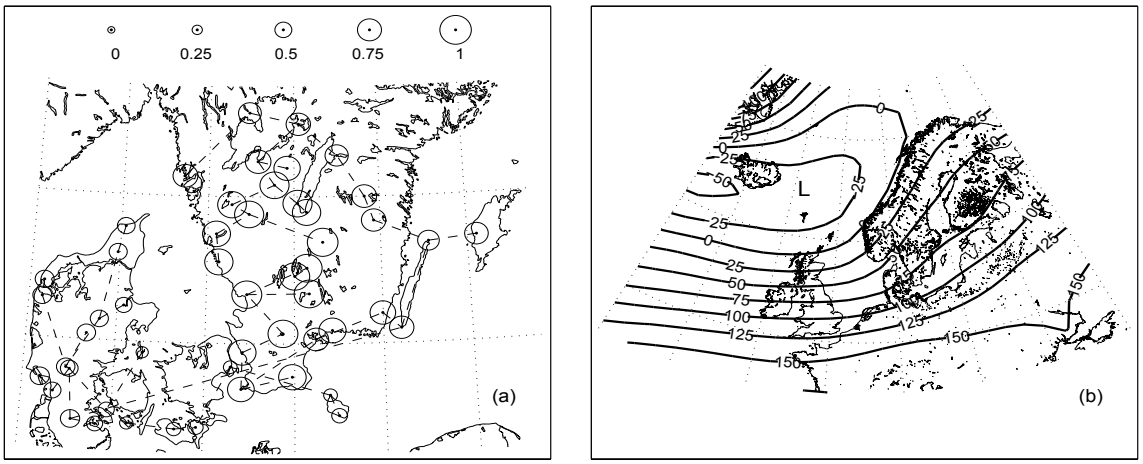

Figure 4.5: Weather state 4: (a) precipitation occurrence probabilities and edges of the Chow-Liu tree; (b) averaged GH-1000 pattern.

Figure 4.7).

State 7 is characterised by a low pressure area over Norway, and thus by prevalent western winds. Precipitation is very likely in Denmark and central Götaland. The small precipitation probabilities in eastern and western Götaland may be correlated to the loss of moisture of the air masses after causing precipitation on the relieves of central Götaland (see Figure 4.8).

State 8 represents weaker westerly conditions than state 7, with lower precipitation probabilities at all gauges, except for those in Jutland and central and western Götaland (see Figure 4.9).

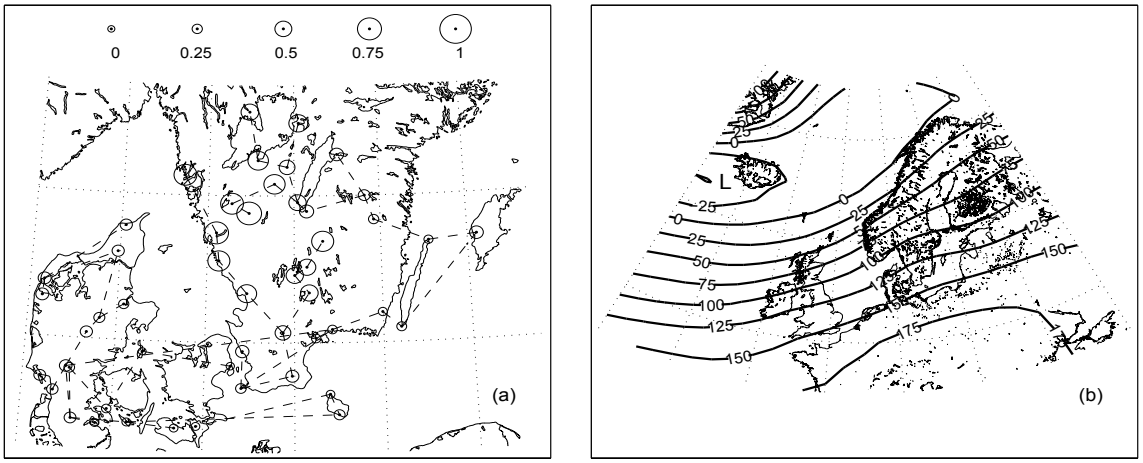

Figure 4.6: Weather state 5: (a) precipitation occurrence probabilities and edges of the Chow-Liu tree; (b) averaged GH-1000 pattern.

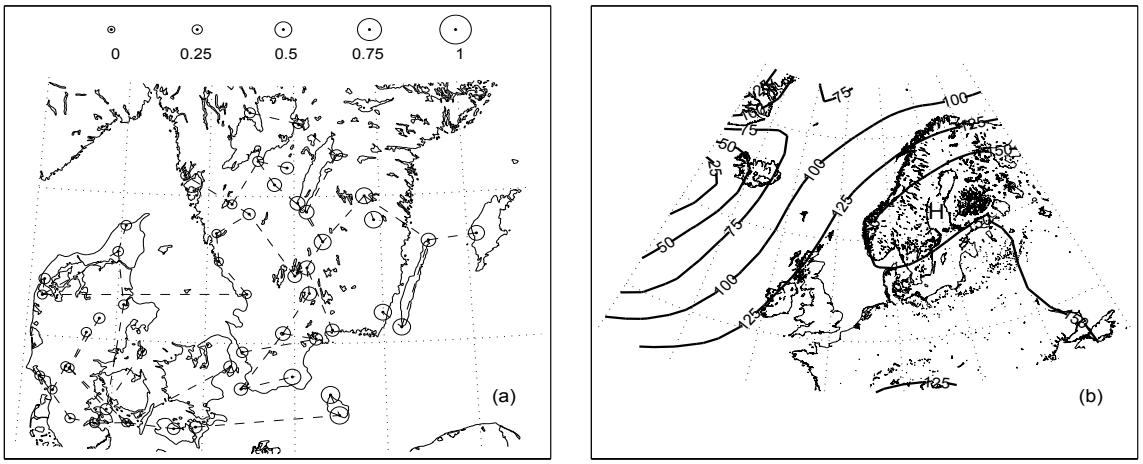

Figure 4.7: Weather state 6: (a) precipitation occurrence probabilities and edges of the Chow-Liu tree; (b) averaged GH-1000 pattern.

To summarise, states 1 and 6 correspond to high pressure weather types; states 3 and 5 may represent either developing or extinguishing low pressure systems; states 4 and 8 correspond to low pressure systems approaching Scandinavia; states 2 and 7 represent fully developed low pressure areas over Scandinavia. In most cases, the model-defined Chow-Liu tree edges connect neighbouring gauges, thus forming likely spatial correlation structures.

The robust predictions of precipitation statistics and the good physical consistency of the weather states may encourage the use of NHMMs for translating large-scale climate change predictions into local-scale precipitation simulations. However, the estimated relations between atmospheric variables and precipitation, which are

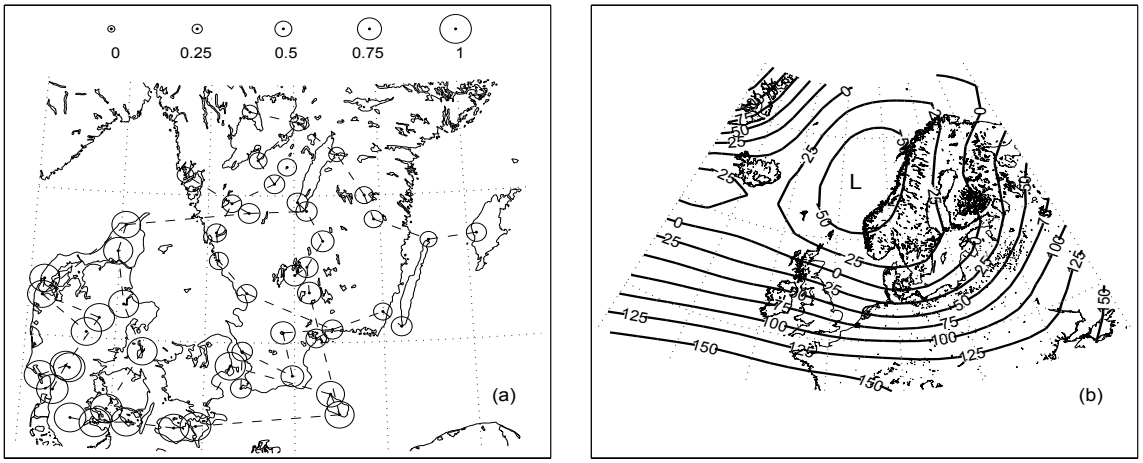

Figure 4.8: Weather state 7: (a) precipitation occurrence probabilities and edges of the Chow-Liu tree; (b) averaged GH-1000 pattern.

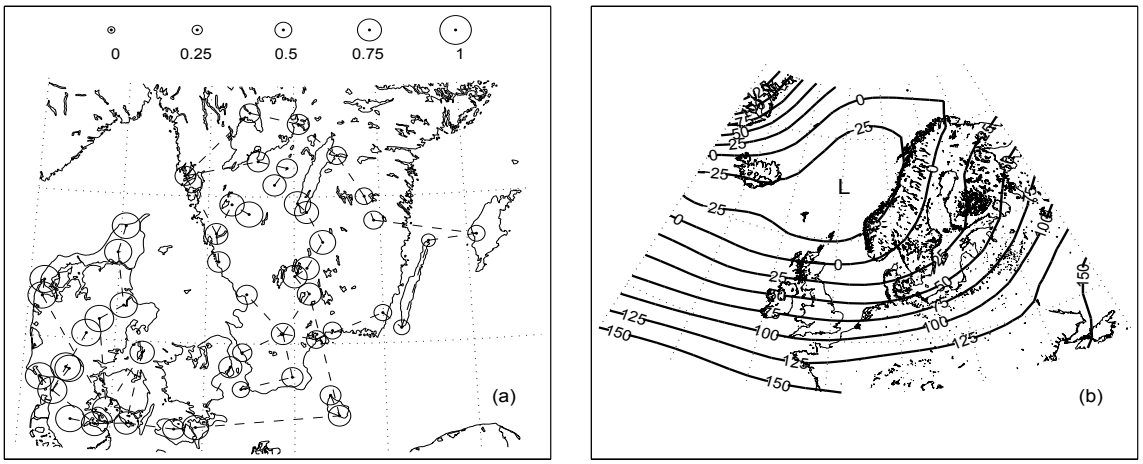

Figure 4.9: Weather state 8: (a) precipitation occurrence probabilities and edges of the Chow-Liu tree; (b) averaged GH-1000 pattern.

valid for past climatic conditions, may not hold under altered climate scenarios.

4.2 Inflow modelling using ENSO information in western Ecuador

In this section we illustrate the application of the MSM defined in section 3.1.2 to model monthly inflow of Daule Peripa using ENSO information. The selected model setup defined 2 climate states and included Niño 1+2 SSTA and TNI as climatic inputs.

The simulated annual inflow data shown in Figure 4.10a derive from monthly val-

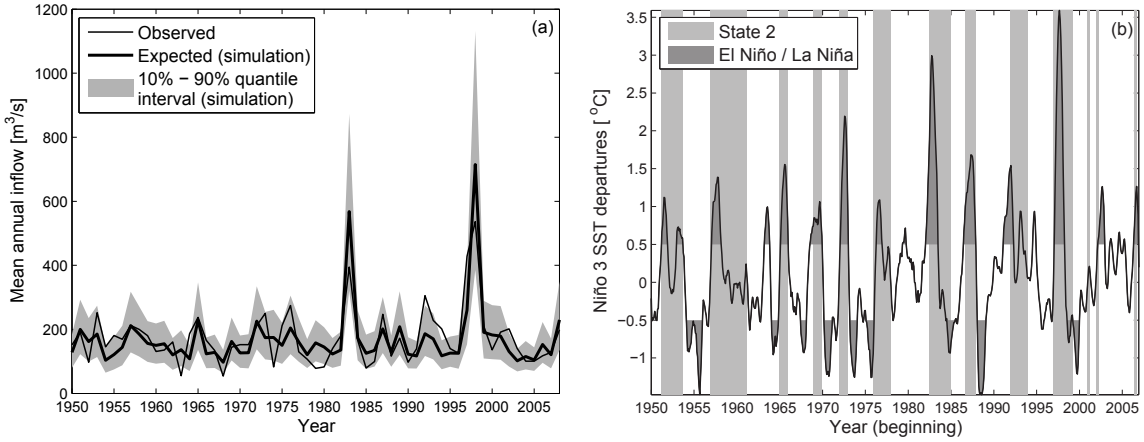

Figure 4.10: (a) Observed and simulated average annual inflow with the 80% quantile interval. (b) Historical ENSO events and inferred occurrences of state 2.

ues generated by conditioning on observed values of ENSO indices. Upwards inflow regime shifts are generally well predicted, except for the largest annual inflow values (in 1983 and 1998), which are overestimated. The 80% quantile interval around the expected value from simulation includes most observations. However, the lowest annual inflow values are systematically overpredicted, due to the small correlation between ENSO indices and negative inflow anomalies.

Figure 4.10b compares the historical El Niño and La Niña events (see section 2.2 for their definition) with the most likely climate state time series inferred by the retrospective analysis. Occurrences of state 2 are well correlated with the observed El Niño events, while state 1 may account for both normal and La Niña conditions. These indications are confirmed by the parameter estimates illustrated in paper I, which discusses in detail the application of the MSM to quarterly inflow of Daule Peripa. Moreover, paper I reports on the reproduction of several inflow statistics, including low- and high-flow duration curves and marginal distributions. By comparing Figures 4.10a and 4.10b, we see that El Niño often associates to anomalously high inflow, while the impact of La Niña does not appear significant.

Figure 4.11 illustrates the expected values of the forecasts performed for 1 and 9 month lead times. Indeed ENSO indices are currently forecasted for lead times up to 9 months. In this application, for the purpose of model testing, we used observed values of ENSO indices instead of forecasts. This constitutes a simplification, and artificially reduces the inflow forecast error. The inflow forecasts show

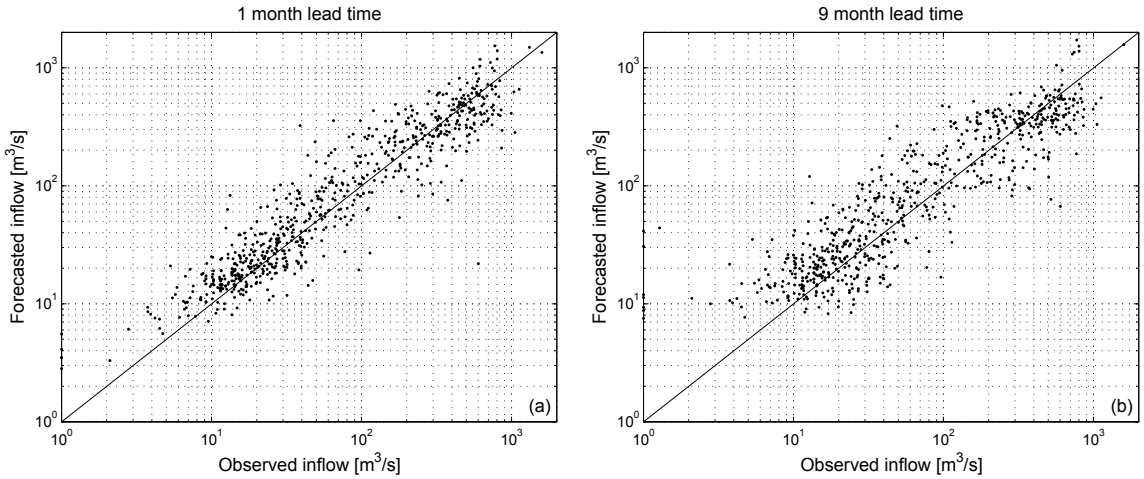

Figure 4.11: Observed monthly inflow versus expected forecasts for (a) 1 and (b) 9 month lead times.

a reasonable fit, although the lowest observed values are slightly overestimated. As expected, the forecast precision decreases with the lead time, even if not dramatically.

The overprediction of anomalously low inflow constitutes the main shortcoming of this modelling application: it might be overcome by pursuing climatic indices that correlate with negative inflow anomalies. As concluded for the downscaling model in section 4.1, applyng the inflow model to predict hydrologic impacts of climate change scenarios may be a risky exercise, despite the robust predictions and the correspondence between climate states and ENSO phases.

4.3 Reservoir optimisation using ENSO information in western Ecuador

The optimisation techniques described in section 3.2 were applied to the Daule Peripa and Baba reservoirs. ENSO-based synthetic inflow time series were used as stochastic input for the reservoir system simulation model defined in section 2.2.2. Section 4.3.2 reports on the application of LT and ST to the Daule Peripa reservoir: the optimised operations were compared to the historical management (HM) and a benchmark solution obtained via the DP algorithm (BS). Section 4.3.2 illustrates the application of ST to the planned Daule Peripa – Baba reservoir system: as no information about the planned operation policy was known, ST was compared to two hypothetical management strategies and BS.

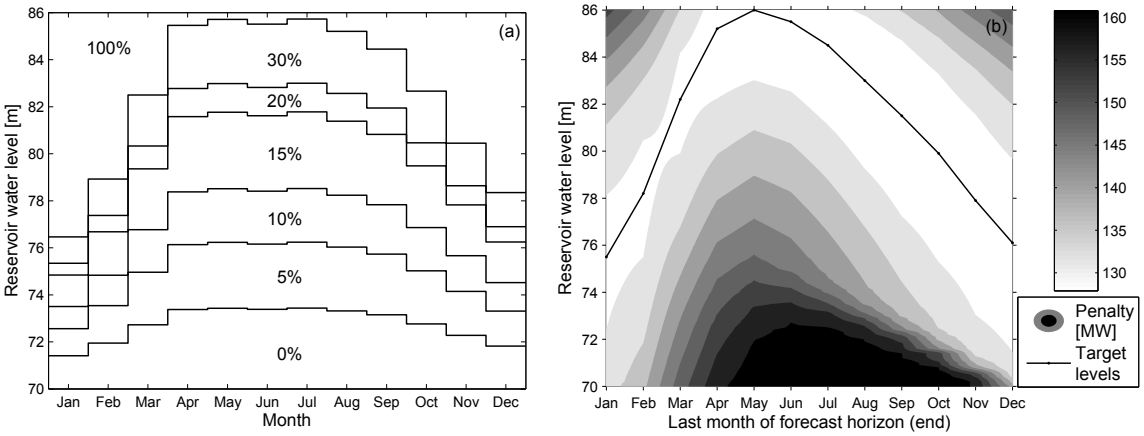

Figure 4.12: Daule Peripa reservoir: (a) rule curves optimised by LT; (b) contour plot of the penalty function with storage targets at the end of the calendar months.

4.3.1 Optimisation of the Daule Peripa reservoir

The rule curves of Daule Peripa were optimised via LT using synthetic inflow, which was simulated by conditioning on observed ENSO indices from 1950 to 1999 (see Figure 4.12a). The pre-defined release fractions were chosen to obtain a set of rule curves characterised by sufficient level resolution and no overlapping. The penalty function, used by ST to account for ERMSHD beyond the 9 month forecast horizon, was mapped by sampling observed inflow from 1950 to 1999. Figure 4.12b reports a contour plot of the estimated penalty values and the storage targets, which are the monthly reservoir water levels minimising the penalty function.

Both storage targets and optimised rule curves indicate the optimal long-term reservoir management: the reservoir should be filled by the end of the wet season to have sufficient storage during the dry months; the reservoir water level at the end of the dry season should be low enough to store the inflow of the following wet season without spills. Spills are defined as non-turbinated releases that do not contribute to satisfying the downstream water demands.

The weight assigned to the penalty term was estimated by performing ST during 1950-1999: ERMSHD was minimised by $\omega = 0.4$. The rule curves optimised by LT and the calibrated ST were applied from 2000 to 2008: Table 4.1 reports performance indicators for HM, LT, ST, and BS. Assuming perfect knowledge of inflow, and given a reservoir water level discretisation, BS approximates the minimum possible ERMSHD conditioned on the satisfaction of the downstream water

Table 4.1: Daule Peripa reservoir: performance indicators for the simulated operations from 2000 to 2008.

	ERMSHD [MW]	Average power [MW]	Downstream deficits [-]	Average spill [m^3/s]
HM	147.0	70.6	0	2.3
LT	144.8	71.4	0	0.9
ST	142.9	73.1	0	1.7
BS	139.8	74.6	0	0

demand. Thus BS was used to benchmark the improvements brought by LT and ST compared to HM: of the maximum ERMSHD reduction estimated by BS, LT and ST yielded 31% and 57%, respectively. LT and ST outperform HM also in terms of average generated power, increasing the production by 1.1% and 3.5%, respectively. No downstream water deficits are observed, thus proving that the optimisation problem was correctly formulated and that efficient turbine releases can satisfy the downstream water demand. Spills are not completely avoided by LT and ST, but are reduced compared to HM.

BS water levels confirm that the theoretical optimal management fills the reservoir at the end of the wet season, and leaves enough empty storage volume at the end of the dry season to store the upcoming wet season inflow (see Figure 4.13a). Such management would avoid spills and preserve high hydraulic heads for hydropower generation. From 2000 to 2002, HM, LT, and ST are relatively close to the optimal management. The low inflow of 2003 causes HM and LT water levels to fall significantly. Instead ST limits dry season releases thanks to the ENSO-based inflow forecasts, and fills the reservoir at the end of the wet season. The anomalously low inflow of 2004 is overpredicted by the stochastic inflow model, thus causing ST water levels to fall. However, ST yields higher water levels than HM and LT, as deviations from monthly storage targets are penalised. Indeed, from 2004 to 2008 we observe LT and HM gradually recovering high hydraulic heads, while ST yields higher water levels at nearly all time steps and is faster at reapproaching the optimal management. LT, which performs better than HM, exploits the information about long-term optimal management held by the rule curves. However, ST outperforms LT, as it combines both short- and long-term information in the form of inflow forecasts and storage targets.

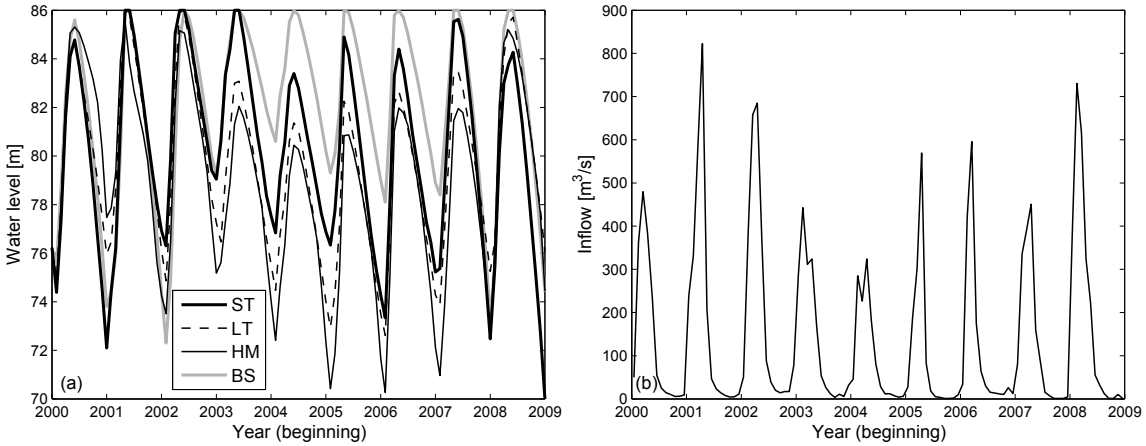

Figure 4.13: Daule Peripa reservoir: (a) water levels of the simulated operations; (b) observed inflow.

To conclude, the integration of climate-driven inflow forecasts with long-term optimal management information yielded the best optimised operation. The potential further improvement shown by BS might be partly achieved by enhancing the quality of inflow forecasts.

A detailed discussion of the long term optimisation minimising two objective functions is available in paper III: the optimisation problem was initially formulated including an objective measuring the downstream deficit, and produced similar results to those presented here. Paper IV illustrates ST results focusing on the benefits yielded by the penalty term.

4.3.2 Optimisation of the Daule Peripa – Baba reservoir system

ST was applied to the planned Daule Peripa – Baba water resources system during 1990-2004, using multivariate inflow forecast scenarios and a penalty term accounting for the water levels of both reservoirs. The ENSO-based inflow forecasts, together with the optimisation results, are discussed in paper IV.

The penalty function was mapped using observed inflow from 1950 to 1989. The resulting storage targets of Daule Peripa were similar to those obtained in section 4.3.2. Conversely, the estimated penalty values did not define any strong preference pattern for Baba, due to its small storage volume (3.5% of the total system capacity). A full discussion of the penalty function for the two reservoir case can be found in paper IV. The optimal value of ω, found by minimising ERMSHD with ST during 1950-1989, was 0.2: the smaller importance of the penalty, compared to

Table 4.2: Daule Peripa – Baba reservoir system: performance indicators for the simulated operations from 1990 to 2004.

	ERMSHD	Average power		Downstream	Average spill	
		Daule Peripa	Baba	deficits	Daule Peripa	Baba
	[MW]	[MW]	[MW]	[-]	[m^3/s]	[m^3/s]
MT	145.6	126.2	18.5	1	64.5	8.6
FR	139.5	125.2	26.8	0	63.4	11.2
ST	135.2	129.0	26.3	1	52.2	11.2
BS	131.3	133.3	26.0	0	44.3	9.6

the single reservoir case, may be due to the water transfer from Baba that facilitates preserving high hydraulic heads at Daule Peripa.

We compared ST to two hypothetical management strategies, assuming that Baba is operated according to a fixed policy, while short-term optimisation is applied only to Daule Peripa: the maximum transfer strategy (MT) maximises the amount of water transferred to Daule Peripa during each time step; the full reservoir strategy (FR) transfers water only if the Baba reservoir is full. Such strategies were conceived to mimic likely sub-optimal operation schemes.

Table 4.2 reports performance indicators of ST, MT, FR, and BS during 1990-2004. ST outperforms MT and FR in terms of both ERMSHD and average power generation. MT minimises the spill from Baba, but yields the lowest hydropower production at Baba due to the low hydraulic heads. Moreover by maximising the amount of transferred water without considering the current storages, MT causes the largest spill from Daule Peripa. Although causing large spills from both reservoirs, FR yields the largest hydropower production at Baba, due to the high hydraulic heads. Compared to MT and FR, ST reduces the spill from Daule Peripa, thus significantly increasing hydropower production. An even larger reduction of the spill from Daule Peripa is yielded by BS, which maximises hydropower production. However, BS does not minimise the spill from Baba, thus implying that minimising the spill from Daule Peripa is decisive for optimising the management.

Spill reduction is achieved by the proper temporal allocation of water transfers from Baba to Daule Peripa: ST determines the releases on the basis of inflow forecasts and current reservoir storages, thus outperforming MT and FR that transferred water without considering the state of Daule Peripa. We can conclude that

the joint reservoir operation implemented by ST enhances the water use efficiency compared to separate management strategies such as MT and FR.

BS reveals that spills cannot be completely avoided. Indeed the inclusion of Baba increases system inflow and storage volume by 60% and 3.5%, respectively. Thus only a small part of the wet season inflow of Baba can be stored and then transferred during the dry season. Moreover the inclusion of Baba may increase the risk of flooding, especially during intense El Niño events. Flood prevention, which was not considered because of the lack of flood vulnerability information, should be included in future analyses.

Table 4.2 shows that ST fails at meeting the downstream water demands once. Adding an objective accounting for the satisfaction of downstream demands would allow analysing the trade-off between hydropower production and water supply reliability. However, such low deficit frequency may not justify the formulation of a multi-objective optimisation problem.

LT and ST, combined with the ENSO-based inflow predictions, might be used to assess the impacts of possible climate change scenarios on the performance of the Daule Peripa – Baba reservoir system. However, the uncertainty involved in such assessment would be large and hardly evaluable, due to the unknown applicability of the modelling approaches under altered climate scenarios.

5 Conclusions

The conducted research focused on the development of stochastic hydrologic models and reservoir optimisation methods that can be beneficially responsive to climatic information.

The description of hydrologic variables such as precipitation and streamflow is conditioned on unobservable (hidden) state variables representing the climatic conditions. We assume the hidden states to be shifting between a finite number of values according to a non-homogeneous Markov chain, in which state transition probabilities are influenced by climatic inputs. The hidden process conditioning the observable variables mimics climate-induced shifts of hydrologic regimes, thus partially accounting for climatic variability.

To test the benefits of climate-responsive hydrologic modelling for water resources management applications, we developed reservoir optimisation methods that can exploit climatic information in the form of climate-based synthetic inflow scenarios.

A non-homogeneous hidden Markov model (NHMM) was applied to downscale synoptic atmospheric patterns to daily precipitation amounts at a dense gauge network in southern Scandinavia. The probability distribution of multivariate precipitation is conditioned on a hidden weather state, whose transition probabilities are functions of gridded atmospheric fields. Although no direct weather classifier is used, the identified weather states exhibit good physical correspondence between their expected precipitation and atmospheric patterns. Moreover, such correspondence validates the summarisation of the highly dimensional atmospheric fields via singular value decomposition. The inclusion of Chow-Liu trees, to approximate the multivariate probability distributions of precipitation occurrences, improves the reproduction of the spatial correlation of precipitation. However, further improvement may be achieved by defining a spatial dependence model for precipitation amounts.

A Markov switching model (MSM) was developed to describe monthly reservoir inflow time series in western Ecuador using El Niño – Southern Oscillation (ENSO) information. Inflow anomalies are modelled by a mixture of autoregressive models with exogenous input (ARX), shifting according to a hidden climate state, whose transitions are influenced by ENSO sea surface temperature indices.

The latter constitute the exogenous input of ARXs, which thus directly include the influence of ENSO on inflow. The developed MSM produces realistic inflow simulations and forecasts based on, respectively, historical records and forecasts of ENSO indices. Monthly ENSO forecasts are currently published for lead times up to 9 months. Due to lack of correlation between ENSO indices and negative inflow anomalies, model calibration identified 2 climate states. Parameter estimates and the inferred most likely historical state sequence indicate that one state corresponds to El Niño, while the other accounts for both normal and La Niña conditions. Model predictions and the correspondence between climate states and ENSO phases reveal that El Niño is well correlated to anomalously high inflow, while the impact of La Niña is not significant. Overprediction of anomalously low inflow constitutes the main shortcoming of this application. Significant improvement might be achieved by pursuing climatic indices that correlate with negative inflow anomalies.

We defined stochastic optimisation methods that could exploit inflow simulations and forecasts performed by the MSM to benefit reservoir operation. The analysed water resources system consists of the Daule Peripa and Baba reservoirs (western Ecuador), which serve hydropower plants and downstream water users. Reservoir operation is optimised according to the simulation-optimisation approach, by coupling a genetic algorithm with a simulation model. Each set of decision variables is evaluated by sampling objective functions on a high number of synthetic inflow scenarios, thus implicitly accounting for input uncertainty. Long-term optimisation (LT) is carried out by calibrating rule curves that return reservoir release as function of current storage and season. Short-term optimisation (ST) is performed at each month by combining long- and short-term information in the form of, respectively, monthly storage targets and inflow forecasts for the following 9 months. LT was applied to the Daule Peripa reservoir, outperforming the historical management (HM). ST was applied to Daule Peripa, outperforming both LT and HM, and then to the planned Daule Peripa – Baba system, for which no designed operation policy is known. The obtained results highlight the benefits of integrating climate-driven inflow forecasts with information about long-term optimal management. As the inclusion of Baba reservoir yields a small increase in storage capacity (3.5%), compared to the average increase in inflow (60%), flood risk mitigation should be considered in future analyses.

The developed methods, ranging from stochastic hydrologic modelling to reser-

voir optimisation, illustrated the potential benefits that may derive from accounting for climatic variability. Modelling approaches produced reasonable predictions by conditioning the description of hydrologic processes on influential climatic phenomena. Reservoir optimisation methods proved the operational improvements that may be achieved by using time series generated by climate-responsive hydrologic models, and by integrating short-term forecasts with information on long-term optimal management. The presented methods might be applied to translate large-scale climate change predictions into small-scale hydrologic impacts, and to derive water resources management policies that perform robustly under climatic variability. However, we must be aware that methods calibrated under past climatic conditions might not be valid for altered climate scenarios.

6 Abbreviations and symbols

ARX ..... autoregressive model with exogenous input.
BS ..... dynamic programming benchmark solution.
CPDF ..... conditional probability density function.
CPMF ..... conditional probability mass function.
DMI ..... Danish Meteorological Institute.
DP ..... dynamic programming.
EM ..... expectation-maximisation.
ENSO ..... El Niño – Southern Oscillation.
ERMSHD ..... expected root mean square hydropower deficit.
ESO ..... explicit stochastic optimisation.
FR ..... full reservoir strategy.
GA ..... genetic algorithm.
GCM ..... general circulation model.
GH-1000 ..... geopotential height at 1000 hPa.
hPa ..... hectopascals.
HM ..... historical management.
ISO ..... implicit stochastic optimisation.
km ..... kilometres.
LP ..... linear programming.
LT ..... long-term optimisation.
m ..... metres.
MRMSHD ..... approximated minimum root mean square hydropower deficit.
MSM ..... Markov switching model.
MT ..... maximum transfer strategy.
MW ..... megawatts.
N ..... north.
NHMM ..... non-homogeneous hidden Markov model.
PAR ..... periodic autoregressive model.
s ..... seconds.
S ..... south.
SO ..... simulation-optimisation.
SST ..... sea surface temperature.
SSTA ..... sea surface temperature anomaly.
ST ..... short-term optimisation.

SVD ..... singular value decomposition.
TNI ..... Trans-Niño Index.
W ..... west.
WCD ..... World Commission on Dams.
WSM ..... weather state model.
$^{\circ}$ ..... arc degrees.
$^{\circ}$C ..... Celsius degrees.
$a_t\,(k)$ ..... observable variables at gauge k at time step t.
$\mathbf{a}_t$ ..... vector of observable variables at time step t.
$\mathbf{a}_{t_1:t_2}$ ..... time series of observable variables from time step t_1 to t_2.
$\widehat{\mathbf{a}}^{(i)}_{t_1:t_2}$ ..... ith synthetic time series of observable variables from time step t_1 to t_2.
$\widehat{\mathbf{A}}^{N}_{t_1:t_2}$ set of N synthetic time series of observable variables from time step t_1 to t_2.
arg ..... argument operator.
$\mathbf{c}_t$ ..... vector of climatic indices at time step t.
$\mathbf{c}_{t_1:t_2}$ ..... time series of climatic indices from time step t_1 to t_2.
$\widehat{\mathbf{c}}_{t_1:t_2}$ ..... forecasted values of climatic indices from time step t_1 to t_2.
cov$\{\cdot\}$ ..... covariance operator.
$\mathbf{D}_t$ ..... diagonal matrix constituted by the elements of $\mathbf{a}_t$.
$\deg(k)$ ..... number of tree edges connecting gauge k.
$\det(\cdot)$ ..... determinant operator.
e ..... typical resolution of a tipping bucket rain gauge (0.2 mm).
E_i ..... Chow-Liu tree for state i.
$\exp(\cdot)$ ..... exponential function.
$f_z(\cdot)$ ..... conditional probability density/mass function of variable z.
$F_{kj}(\cdot)$ .. conditional bivariate discrete distribution of precipitation occurrences at gauges k and j.
$F_k(\cdot)$ ..... marginalisation of $F_{kj}(\cdot)$ with respect to any $j \neq k$.
g_t ..... average power generated by the hydropower plants during time step t.
$\widehat{g}^{(i)}_{t_1:t_2}$. ith simulated hydropower time series from time step t_1 to t_2, corresponding to $\mathbf{q}^{(i)}_{t_1:t_2}$.
$\widehat{\mathbf{g}}^{N}_{t_1:t_2}$ ..... set of N simulated hydropower time series from time step t_1 to t_2, corresponding to $\widehat{\mathbf{Q}}^{N}_{t_1:t_2}$.
G ..... power demand, set equal to the sum of all turbine power capacities.
Ga$(\cdot\,;\xi_{ki},\varphi_{ki})$ two parameter Gamma probability density function with parameters ξ_{ki} and φ_{ki}.
$h^k(x)$ ..... water level of reservoir k at time x.

$\overline{h}_t^i$ ..... average water level of reservoir i during time step t.

$\mathbf{h}_t$ ..... vector of reservoir water levels at the end of time step t.

$\widehat{\mathbf{h}}_{t+l}^{(n)}$ vector of reservoir water levels at the end of $t+8$, obtained by implementing $\boldsymbol{\rho}_{t:t+l}$ given $\widehat{\mathbf{q}}_{t:t+l}^{(n)}$.

h_{min}^k ..... minimum operational water level of reservoir k.

h_{max}^k ..... maximum operational water level of reservoir k.

$\mathbf{H}_{LT}$ .....complete set of decision variables for long-term optimisation.

k_t^i ..tailwater height downstreams of the hydropower plant supplied by reservoir i during time step t.

$L(\cdot)$ ..... model likelihood function.

$m(t)$ ..... function returning the calendar month corresponding to time step t.

$\max\{\cdot\}$ .....maximisation operator.

o_{ki} .....precipitation occurrence probability at gauge k for state i.

p_{ij} .....stationary component of the transition probability from state i to j.

$P(\cdot)$ ..... penalty function (short-term optimisation).

$\Pr\{\cdot\}$ ..... probability operator.

$\widehat{\mathbf{q}}_{t_1:t_2}^{(i)}$ ..... ith synthetic inflow time series from time step t_1 to t_2.

$\widehat{\mathbf{Q}}_{t_1:t_2}^{N}$ .....set of N synthetic inflow time series from time step t_1 to t_2.

r_t^i ..... turbine release of reservoir i during time step t.

R^i ....turbine hydraulic capacity of the hydropower plant supplied by reservoir i.

$\widehat{\mathbf{r}}_{t_1:t_2}^{(i)}$ ..... ith simulated turbine release time series from time step t_1 to t_2, corresponding to $\mathbf{q}_{t_1:t_2}^{(i)}$.

$\widehat{\mathbf{R}}_{t_1:t_2}^{N}$ .....set of N simulated turbine release time series from time step t_1 to t_2, corresponding to $\widehat{\mathbf{Q}}_{t_1:t_2}^{N}$.

s_t ..... hidden state at time step t.

$\mathbf{s}_{t_1:t_2}$ ..... time series of hidden states from time step t_1 to t_2.

s_t^* .....most likely hidden state at time step t, given observations and model parameters.

$\mathbf{s}_{t_1:t_2}^*$ .....most likely time series of hidden states from time step t_1 to t_2, given observations and model parameters.

q_t^i .....inflow of reservoir i during time step t.

$v^i(x)$ ..... storage volume of reservoir i at time x.

$\mathbf{V}$ .....scale matrix, set equal to the covariance matrix of $\mathbf{c}_t$.

w_t^i .....downstream release of reservoir i during time step t.

W^i .....water demand of the downstream users from reservoir i.

$\boldsymbol{\phi}_i$ ..... diagonal matrix, whose non-null elements are the eigenvalues of $\boldsymbol{\Omega}_i$.

$y(\cdot)$ ..... objective function for long-term optimisation.
$Y(\cdot)$ ..... objective function for short-term optimisation.
$\alpha_t(k)$ ..... precipitation occurrence at gauge k on day t.
$\boldsymbol{\alpha}_t$ ..... precipitation occurrence pattern on day t.
$\boldsymbol{\beta}_t$ ..... vector of conditioning variables at time step t.
$\boldsymbol{\Gamma}_i$ ..... vector of exogenous correlation ARX parameters for state i.
$\boldsymbol{\delta}_i$ ..... vector of intercept ARX parameters for state i.
ε^i ..... turbine efficiency of the hydropower plant supplied by reservoir i.
$\boldsymbol{\varepsilon}_t$ ..... vector of standard Gaussian independent white noise processes.
$eta_u^k(i)$ ..... upper water level bound for the uth pre-defined release fraction of reservoir k during calendar month i.
$\boldsymbol{\eta}_u^k = \left\{\eta_u^k(1), \ldots, \eta_u^k(12)\right\}$ ..... uth rule curve of reservoir k.
$\boldsymbol{\theta}$ ..... model parameters set.
$\boldsymbol{\lambda}_i$ ..... vector of autoregressive ARX parameters for state i.
$\boldsymbol{\mu}_i$ ..... value of $\mathbf{c}_t$ maximising the probability of shifting to state i.
$\boldsymbol{\Xi}_i$ ..... matrix, whose columns are the eigenvectors of $\boldsymbol{\Omega}_i$.
ρ_t^i ..... turbine release fraction of reservoir i during time step t.
$\rho^k(x)$ ..... actual turbine release fraction of reservoir k at time x.
$\boldsymbol{\rho}_t$ ..... vector of turbine release fractions of all reservoirs during time step t.
$\boldsymbol{\rho}_{t_1:t_2}$ time series of turbine release fractions of all reservoirs from time step t_1 to t_2.
τ_t ..... end time of time step t.
υ_u^k ..... uth pre-defined release fraction.
ϕ ..... specific weight of water.
χ_{u-1}^k ..... scaling factor defining the uth rule curve of reservoir k.
$\boldsymbol{\psi}_1$ ..... auxiliary vector for computing model likelihood.
$\boldsymbol{\Psi}_t$ ..... auxiliary matrix for computing model likelihood.
$\boldsymbol{\Omega}_i$ ..... matrix of covariance ARX parameters for state i.
ω ..... weight assigned to the penalty function (short-term optimisation).

7 References

Akintuğ, B., and P. F. Rasmussen, A Markov switching model for annual hydrologic time series, *Water Resources Research*, *41*(9), W09424, doi: 10.1029 / 2004WR003605, 2005.

Bardossy, A., and E. J. Plate, Modeling daily rainfall using a semi-Markov representation of circulation pattern occurrence, *Journal of Hydrology*, *122*(14), 33-47, 1991.

Bates, B. C., S. P. Charles, and J. P. Hughes, Stochastic downscaling of numerical climate model simulations, *Environmental Modelling & Software*, *13*(34), 325-331, 1998.

Baum, L. E., T. Petrie, G. Soules, and N. Weiss, A maximization technique occurring in the statistical analysis of probabilistic functions of Markov chains, *The Annals of Mathematical Statistics*, *41*(1), 164–171, doi: 10.1214 / aoms / 1177697196, 1970

Bellman, R., *Dynamic programming*, Princeton University Press, Princeton, NJ, USA, 1957.

Bellone, E., J. P. Hughes, and P. Guttorp, A hidden Markov model for downscaling synoptic atmospheric patterns to precipitation amounts, *Climate Research*, *15*(1), 1–12, doi: 10.3354 / cr015001, 2000.

Bertsekas, D., *Dynamic Programming and Optimal Control*, AthenaScientific, Belmont, MA, USA, 2000.

Bretherton, C. S., C. Smith, and J. M. Wallace, An intercomparison of methods for finding coupled patterns in climate data, *Journal of Climate*, *5*(4), 541-560, 1992.

Cappè, O., E. Moulines, and T. Rydèn (Eds.), *Inference in Hidden Markov Models*, Springer Series in Statistics, New York, NY, 2005.

Celeste, A. B., K. Suzuki, and A. Kadota, Integrating long- and short-term reservoir operation models via stochastic and deterministic optimization: case study in

Japan, *Journal of Water Resources Planning and Management*, *134*(5), 440–448, 2008.

Charles, S. P., B. C. Bates, P. H. Whetton, and J. P. Hughes, Validation of downscaling models for changed climate conditions: case study of southwestern Australia, *Climate Research*, *12*(1), 1-14, 1999.

Chen, L., Real coded genetic algorithm optimisation of long term reservoir operation, *Journal of the American Water Resources Association*, *39*(5), 1157–1165, 2003.

Chow, C. K., and C. N. Liu, Approximating discrete probability distributions with dependence trees, *IEEE Transactions on Information Theory*, *14*(3), 462-467, 1968.

Dempster, A. P., N. M. Laird, and D. B. Rubin, Maximum likelihood from incomplete data via the EM algorithm, *Journal of the Royal Statistical Society Series B-Methodological*, *39*(1), 1–38, 1977.

DMI, *Vejr for enhver – Vejr, klima og miljø*. Danish Meteorological Institute, Copenhagen, Denmark, 1997.

Cooke, D. S., The duration of wet and dry spells at Moncton, New-Brunswick, *Quarterly Journal of the Rroyal Meteorological Society*, *79*(342), 536–538, 1953.

Fortin, V., L. Perrault, and J. D. Salas, Retrospective analysis and forecasting of streamflows using a shifting level model, *Journal of Hydrology*, *296*(1-4), 135–163, 2004.

Georgakakos, A., The value of streamflow forecasting in reservoir operation, *Water Resources Bulletin*, *25*(4), 789–800, 1989.

Giorgi, F., and L. O. Mearns, Approaches to the simulation of regional climate change: a review, *Reviews of Geophysics*, *29*(2), 191-216, 1991.

Goldberg, D. E., *Genetic Algorithms in Search, Optimization, and Machine Learning*, Addison-Wesley, Reading, MA, 1989.

Gopalakrishnan, G., B. S. Minsker, and D. Goldberg, Optimal sampling in a noisy

genetic algorithm for risk-based remediation design, in *Bridging the gap: meeting the worlds water and environmental resources challenges. Proc world water and environmental resources congress*, edited by D. Phelps and G. Sehlke, ASCE, Washington DC (USA), 2001.

Grantz, K., and B. Rajagopalan, A technique for incorporating large-scale climate information in basin-scale ensemble streamflow forecasts, *Water Resources Research*, *41*, W10410, doi: 10.1029 / 2004WR003467, 2005.

Green, J. R., A generalised probability model for sequences of wet and dry days, *Monthly Weather Review*, *98*, 238–241, 1970.

Haan, C. T., D. M. Allen, and J. O. Street, A Markov chain model of daily rainfall, *Water Resources Research*, *12*(3), 443-449, 1976.

Hamilton, J. D., A new approach to the economic analysis of nonstationary time series and the business cycle, *Econometrica*, *57*(2), 357–384, 1989.

Hay, E. L., G. J. McCabe, D. M. Wolock, and M. A. Ayers, Simulation of precipitation by weather type analysis, *Water Resources Research*, *27*(4), 493-501, 1991.

Hipel, K. W., and A. I. McLeod (Eds.), *Time Series Modelling of Water Reources and Environmental Systems*, Elsevier, New York, 1994.

Holland, J. H., *Adaptation in Natural and Artificial Systems*, Massachussets Institute of Technology, Cambridge, 1992.

Hughes, J. P., and P. Guttorp, A class of stochastic models for relating synoptic atmospheric patterns to regional hydrologic phenomena, *Water Resources Research*, *30*(5), 1535-1546, 1994.

Hughes, J. P., P. Guttorp, and S. P. Charles, A non-homogeneous hidden Markov model for precipitation occurrence, *Journal of the Royal Statistical Society*, *48*(1), 15–30, doi: 10.1111 / 1467-9876.00136, 1999.

Hughes, J. P., D. P. Lettenmaier, and P. Guttorp, A stochastic approach for assessing the effect of changes in synoptic circulation patterns on gauge precipitation,

Water Resources Research, *29*(10), 3303-3315, 1993.

Kapelan, Z., D. A. Savic, G. A. Walters, and A. V. Babayan, Risk- and robustness-based solutions to a multi-objective water distribution system rehabilitation problem under uncertainty, *Water Science & Technology*, *53*(1), 61–75, 2006.

Karamouz, M., and M. H. Houck, Comparison of stochastic and deterministic dymnamic programming for reservoir operating rule generation, *Journal of the American Water Resources Association*, *23*(1), 1–9, 1987.

Kelman, J., A. M. Vieira, and J. E. Rodriguez-Amaya, El Niño influence on streamflow forecasting, *Stochastic Environmental Research and Risk Assessment*, *14*(2), 123–138, 2000.

Kirshner, S., P. Smyth, and A. W. Robertson, Conditional ChowLiu tree structures for modeling discrete-valued time series, *Proceedings of the 20th Annual Conference on Uncertainty in Artificial Intelligence (UAI-04)*. AUAI Press, Arlington, VA, 317-324, 2004.

Labadie, J., R. Lazaro, and D. Morrow, Worth of short-term rainfall forecasting for combined sewer overflow control, *Water Resources Research*, *17*(6), 1594–1604, 1981.

Labadie, J. W., Optimal operation of multireservoir systems: state-of-the-art review, *Journal of Water Resources Planning and Management*, *130*(2), 93–111, 2004.

Landman, W. A., S. J. Mason, and W. J. Tennant, Statistical downscaling of GCM simulations to streamflow, *Journal of Hydrology*, *252*(1-4), 221–236, doi: 10.1016 / S0022-1694(01)00457-7, 2001.

Linderson, M.-L., Objective classification of atmospheric circulation over southern Scandinavia, *International Journal of Climatology*, *21*(2), 155–169, 2001.

Lu, Z.-Q., and L. M. Berliner, Markov switching time series models with application to a daily runoff time series, *Water Resources Research*, *35*(2), 523–534, 1999.

MacDonald, I. L., and W. Zucchini (Eds.), *Hidden Markov and Other Models for Discrete-Valued Time Series*, CRC Press, Boca Raton, FL, 1997.

Meila, M., M. I. Jordan, Learning with mixtures of trees, *Journal of Machine Learning Research*, *1*(1), 148, 2000.

Mishalani, N., and N. Palmer, Forecast uncertainty in water supply reservoir operation, *Water Resources Bulletin*, *24*(6), 1237–1245, 1988.

Mujumdar, P. P., and T. S. V. Ramesh, Real-time reservoir operation for irrigation, *Water Resources Research*, *33*(5), 1157–1164, 1997.

Mujumdar, P. P., and T. S. V. Ramesh, A short-term reservoir operation model for multicrop irrigation, *Hydrological Sciences Journal*, *43*(3), 479–494, 1998.

Ngo, L. L., H. Madsen, and D. Rosbjerg, Simulation and optimisation modelling approach for operation of the hoa binh reservoir, *Journal of Hydrology*, *336*(3–4), 269-281, 2007.

Oliveira, R., and D. P. Loucks, Operating rules for multi-reservoir systems, *Water Resources Research*, *33*(4), 839–852, 1997.

Piechota, T. C., and J. A. Dracup, Long-range streamflow forecasting using El Niño-Southern Oscillation indicators, *Journal of Hydrologic Engineering*, *4*(2), 144–151, doi: 10.1061 / (ASCE)1084-0699(1999)4:2(144), 1999.

Rabiner, L. R., A tutorial on hidden Markov models and selected applications in speech recognition, *Proceedings of the IEEE*, *77*(2), 257–286, 1989.

Rani, D., and M. M. Moreira, Simulation-optimization modeling: a survey and potential application in reservoir systems operation, *Water Resources Management*, *24*(6), 1107–1138, 2009.

Robertson, A. W., S. Kirshner, and P. Smyth, Downscaling of daily rainfall occurrence over northeast Brazil using a hidden Markov model, *Journal of Climate*, *17*(22), 4407–4424, doi: 10.1175 / JCLI-3216.1, 2004.

Robertson, A. W., A. V. M. Ines, and J. W. Hansen, Downscaling of seasonal pre-

cipitation for crop simulation, *Journal of Applied Meteorology and Climatology*, *46*, 677-693, 2007.

Roefs, T., and T. Bodin, Multireservoir operation studies, *Water Resources Research*, *6*(2), 410–420, 1970.

Salas, J. D., Analysis and modeling of hydrologic time series (Chapter 19), in *Handbook of Hydrology*, edited by D. R. Maidment, McGraw-Hill, New York, 1993.

Sharif, M., and R. Wardlaw, Multireservoir systems optimisation using genetic algorithms: case study, *Journal of Computing in Civil Engineering*, *14*(4), 255–263, 2000.

Simonovic, S. P., and D. H. Burn, An improved methodology for short-term operation of a single multipurpose reservoiran improved methodology for short-term operation of a single multipurpose reservoir, *Water Resources Research*, *25*(1), 1–8, 1989.

Simonovic, S. P., Reservoir systems analysis: closing gap between theory and practice, *Journal of Water Resources Planning and Management*, *118*(3), 262-80, 1992.

Smalley, J. B., and B. S. Minsker, Risk-based in situ bioremediation design using a noisy genetic algorithm, *Water Resources Research*, *36*(10), 3043–3052, 2000.

Stern, R. D., and R. Coe, A model fitting analysis of daily rainfall data. *Journal of Royal Statistical Society Series A*, *147*(1), 1-34, 1984.

Tickle, K. S., and I. C. Goulter, Uncertainty in reservoir operation optimisation, in *Water Policy and Management: Solving the Problems*, edited by D. G. Fontane and H. N. Tuvel, pp. 3043–3052, ASCE, New York (USA), 1994.

Trenberth, K. E., The definition of El Niño, *Bulletin of the American Meteorological Society*, *78*(12), 2771–2777, 1997.

Trenberth, K. E., and D. P. Stepaniak, Indices of El Niño evolution, *Journal of Climate*, *14*(8), 1697–1701, doi: 10.1175 / 1520-0442(2001)014 < 1697:LIOENO > 2.0.CO;2, 2001.

Uvo, C. B., and N. E. Graham, Seasonal runoff forecast for northern South America: a statistical model, *Water Resources Research*, *34*(12), 3515–3524, 1998.

Viterbi, A. J., Error bounds for convolutional codes and an asymptotically optimum decoding algorithm, *IEEE Transactions on Information Theory*, *13*(2), 260–269, 1967.

Vuille, M., R. S. Bradley, and F. Keimig, Climate variability in the Andes of Ecuador and its relation to tropical Pacific and Atlantic sea surface temperature anomalies, *Journal of Climate*, *13*(14), 2520–2535, 1999.

WCD, *World Commission on Dams. Dams and development: a new framework for decision-making*, Earthscan Publications Ltd, 2000.

Wu, J., C. Zheng, C. C. Chien, and L. Zheng, A comparative study of Monte Carlo simple genetic algorithm and noisy genetic algorithm for cost-effective sampling network design under uncertainty, *Advances in Water Resources*, *29*(6), 899–911, 2006.

Wurbs, R. A., Reservoir-system simulation and optimization models, *Journal of Water Resources Planning and Management*, *119*(4), 455–472, 1993.

Yeh, W., Reservoir management and operations models: a state-of-the-art review, *Water Resources Research*, *21*(12), 1797–1818, 1985.

Zucchini, W., and P. Guttorp, A hidden Markov model for space-time precipitation, *Water Resources Research*, *27*(8), 1917-1923, 1991.

8 Appendices

I. Gelati, E., O. B. Christensen, P. F. Rasmussen, and D. Rosbjerg, Downscaling atmospheric patterns to multi-site precipitation amounts in southern Scandinavia, *Hydrology Research*, *41*(3-4), 193–210, doi: 10.2166 / nh.2010.114, 2010.

II. Gelati, E., H. Madsen, and D. Rosbjerg, Markov-switching model for non-stationary runoff conditioned on El Niño information, *Water Resources Research*, *46*, W02517, doi: 10.1029 / 2009WR007736, 2010.

III. Gelati, E., H. Madsen, and D. Rosbjerg, Stochastic reservoir optimisation using El Niño information – case study of Daule Peripa, Ecuador, revised to *Hydrology Research*.

IV. Gelati, E., H. Madsen, and D. Rosbjerg, Reservoir operation using El Niño forecasts, submitted manuscript.

The papers are not included in this www-version, but can be obtained from the Library at DTU Environment:
Department of Environmental Engineering
Technical University of Denmark
Miljøvej, Building 113
DK-2800 Kongens Lyngby, Denmark
(library@env.dtu.dk)

The Department of Environmental Engineering (DTU Environment) conducts science-based engineering research within four themes:
Water Resource Engineering, Urban Water Engineering,
Residual Resource Engineering and Environmental Chemistry & Microbiology.
Each theme hosts two to five research groups.

The department dates back to 1865, when Ludvig August Colding, the founder of the department, gave the first lecture on sanitary engineering as response to the cholera epidemics in Copenhagen in the late 1800s.

DTU Environment
Department of Environmental Engineering
Technical University of Denmark

Miljoevej, building 113
DK-2800 Kgs. Lyngby
Denmark

Phone: +45 4525 1600
Fax: +45 4593 2850
e-mail: reception@env.dtu.dk
www.env.dtu.dk

ISBN 978-87-92654-09-0